ABSORBING BOUNDARY CONDITIONS FOR RAYLEIGH WAVES*

ALAIN BAMBERGER†‡, BRUNO CHALINDAR§, PATRICK JOLY†,
JEAN ELIZABETH ROBERTS†, AND JEAN LUC TERON¶

Abstract. The first-order absorbing boundary conditions for elastic waves are transparent for P and S waves at normal incidence, but give rise to parasitic reflections of Rayleigh waves. To treat these phenomena, a solution of geometric type is proposed that eliminates these parasitic waves but causes others to appear, which, while less important, are still troublesome. A second solution is proposed by constructing a new condition of second-order type, transparent for P and S waves at normal incidence as well as for Rayleigh waves. This condition is analyzed mathematically and its good behavior is demonstrated with regard to reflection phenomena.
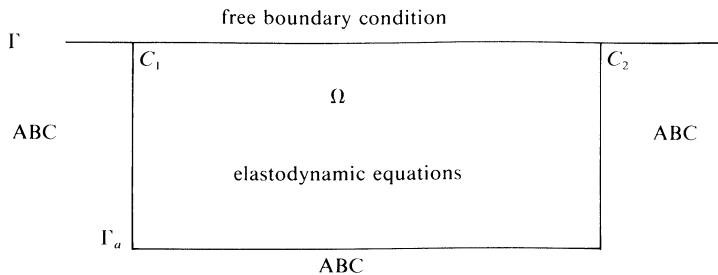
Key words. absorbing boundary conditions, elastodynamics, Rayleigh waves

AMS(MOS) subject classifications. 86-08, 73D20, 35L20, 65N99

Résumé. Les conditions absorbantes du premier ordre pour les ondes élastiques sont transparentes pour les ondes P et S à incidence normale mais font apparaître des réflexions d'ondes de Rayleigh parasites. Pour éliminer ces phénomènes, nous proposons une première solution de type géométrique, qui permet de réduire l'amplitude des ondes parasites mais en fait naître de nouveaux, de moindre importance (quoique toujours gênants). Nous proposons une seconde solution en construisant une nouvelle condition, type second ordre, transparente pour les ondes P et S à incidence normale et pour les ondes de Rayleigh. Nous analysons mathématiquement cette condition et mettons en évidence ses bonnes propriétés vis à vis des phénomènes de réflexion.

Mot clés. conditions aux bords absorbantes, ondes élastiques, ondes de Rayleigh

Introduction. We are interested here in the problem of constructing absorbing boundary conditions for linear elastodynamic equations in the two-dimensional half space with free boundary condition. The objective is to reduce the domain of calculation to a bounded open set Ω using artificial absorbing boundary conditions (ABCs) on the artificial boundary Γ_a. Such absorbing conditions must be constructed so as to minimize the parasitic reflections that will occur. Solutions to the problem exist for equations in the whole space for the wave equation [2], [4], [6], for the Navier–Stokes equations [9], and for linear elastodynamic equations [4]-[8]. In fact, it is well known that classical first-order boundary conditions for elastodynamic equations in the whole space have good transparency properties with respect to pressure and shear waves.

In the half space, on the contrary, the Rayleigh waves, which propagate along the free boundary Γ, are reflected by the artificial boundary when they reach the intersection points with the free boundary (i.e., points C_1 and C_2 on the above figure). This is a parasitic phenomenon whose amplitude, while not exceedingly strong, is of sufficient importance to be troublesome for applications in geophysics. To our knowledge no author has yet directly attacked this problem; however, we point out that in [5], the reflection of Rayleigh waves is studied but only for ABCs designed for the elastodynamic equations in the whole space. In this article, we analyze this phenomenon of the reflection of Rayleigh waves and propose different solutions to the problem.

1. Reflection of Rayleigh waves by the first-order condition.

1.1. The first-order absorbing boundary condition and its properties. Let us recall the linear elastodynamic equations in a nonviscous isotropic two-dimensional medium,

$$\rho\frac{\partial^2 u_1}{\partial t^2}-\frac{\partial}{\partial x_1}\left(\lambda\left(\frac{\partial u_1}{\partial x_1}+\frac{\partial u_2}{\partial x_2}\right)+2\mu\frac{\partial u_1}{\partial x_1}\right)-\frac{\partial}{\partial x_2}\left(\mu\left(\frac{\partial u_1}{\partial x_2}+\frac{\partial u_2}{\partial x_1}\right)\right)=0,$$

$$\rho\frac{\partial^2 u_2}{\partial t^2}-\frac{\partial}{\partial x_1}\left(\mu\left(\frac{\partial u_1}{\partial x_2}+\frac{\partial u_2}{\partial x_1}\right)\right)-\frac{\partial}{\partial x_2}\left(\lambda\left(\frac{\partial u_1}{\partial x_1}+\frac{\partial u_2}{\partial x_2}\right)+2\mu\frac{\partial u_2}{\partial x_2}\right)=0.$$

Here, $u_1(x_1, x_2, t)$ and $u_2(x_1, x_2, t)$ denote the horizontal and vertical components of the displacement vector $U(x_1, x_2, t)$ of a particle whose coordinates are x_1 and x_2. The density of the material is denoted by $\rho(x_1, x_2)$, and $\lambda(x_1, x_2)$ and $\mu(x_1, x_2)$ are its Lamé coefficients.

When the medium is homogeneous (ρ, λ, and μ are constant), any physical solution in the whole space $\mathbb{R}^2$ can be decomposed as the superposition of harmonic plane waves, i.e., solutions in the form

$$U(x_1, x_2, t) = U_D \exp i(\omega t - k_1 x_1 - k_2 x_2),$$

where U_D is the displacement vector, ω is the pulsation, and $k = (k_1, k_2)$ is the wave vector.

It is well known that there exist two kinds of such plane waves:

(1) The P waves characterized by the two following properties:
    (a) The displacement vector U_D is parallel to the wave vector k,
    (b) The wave propagates with the velocity

$$V_P = \frac{\omega}{|k|} = \left(\frac{\lambda+2\mu}{\rho}\right)^{1/2}, \qquad (|k| = (k_1^2 + k_2^2)^{1/2}).$$

(2) The S waves characterized by the following two properties:
    (a) The displacement vector U_D is orthogonal to the wave vector k;
    (b) The wave propagates with the velocity

$$V_S = \frac{\omega}{|k|} = \left(\frac{\mu}{\rho}\right)^{1/2}.$$

Now let Γ be an artificial boundary of a domain Ω of calculation and n be the exterior unit normal vector to Γ.

We recall that a classical first-order absorbing boundary condition for the elastodynamic equations is given by [5]

$$(1.1) \qquad\qquad \sigma \cdot n + M\frac{\partial u}{\partial t} = 0,$$

where $\sigma(x_1, x_2, t)$ denotes the stress tensor:

$$\sigma_{11} = \lambda \left(\frac{\partial u_1}{\partial x_1} + \frac{\partial u_2}{\partial x_2} \right) + 2\mu \frac{\partial u_1}{\partial x_1},$$

$$\sigma_{22} = \lambda \left(\frac{\partial u_1}{\partial x_1} + \frac{\partial u_2}{\partial x_2} \right) + 2\mu \frac{\partial u_2}{\partial x_2},$$

$$\sigma_{12} = \sigma_{21} = \mu \left(\frac{\partial u_1}{\partial x_2} + \frac{\partial u_2}{\partial x_1} \right),$$

and where $M = M(x_1, x_2)$ is the matrix

$$(1.2) \qquad M = \begin{pmatrix} n_1 & n_2 \\ n_2 & -n_1 \end{pmatrix} \cdot \begin{pmatrix} \rho V_P & 0 \\ 0 & \rho V_S \end{pmatrix} \cdot \begin{pmatrix} n_1 & n_2 \\ n_2 & -n_1 \end{pmatrix}.$$

Note that the matrix M is symmetric and positive definite; thus, the boundary condition expresses the fact that at the boundary, the normal stress on Γ is directly proportional to the velocity.

By construction, the condition (1.1), (1.2) is the unique condition of type (1.1), with M symmetric and positive definite, which is transparent for all plane harmonic P and S waves arriving at Γ with normal incidence (this means that plane waves P and S automatically satisfy (1.1) as soon as the wave vector k is parallel to n). Note also that for each displacement field u satisfying the equations of elastodynamics in Ω and a condition of type (1.1) on Γ, with M symmetric and positive definite, we have the energy identity:

$$(1.3) \qquad \frac{1}{2} \frac{d}{dt} \{E(\Omega, t)\} + \int_\Gamma M \frac{\partial u}{\partial t} \cdot \frac{\partial u}{\partial t} \, d\gamma = 0,$$

where $E(\Omega, t)$, which is given by

$$E(\Omega, t) = \frac{1}{2} \int_\Omega \rho \left| \frac{\partial u}{\partial t} \right|^2 dx + \frac{1}{2} \int_\Omega \lambda |\mathrm{div}\, u|^2 \, dx + \int_\Omega \mu \left(\frac{\partial u_i}{\partial x_j} + \frac{\partial u_j}{\partial x_i} \right)^2 dx,$$

denotes the total energy of the field u contained at instant t in the domain Ω. Let us recall that, thanks to Korn's inequality, we have

$$E(\Omega, t) \geqq \frac{1}{2} \int_\Omega \rho \left| \frac{\partial u}{\partial t} \right|^2 dx + C(\Omega) \left(\sum_{j=1}^{2} \left(\int_\Omega |\nabla u_j|^2 \, dx \right) - \int_\Omega |u|^2 \, dx \right).$$

The equality (1.3) implies, in particular, that the total energy is a nonincreasing function of time, i.e., any boundary condition of type (1.1) is an absorbing condition and thus leads to a well-posed mathematical problem.

We summarize these well-known properties in the following theorem.

THEOREM 1.1. *Formula (1.1), where M is a symmetric, positive definite matrix, defines a family of absorbing boundary conditions for the equations of elastodynamics in two dimensions. If M is given by (1.2), the resulting boundary condition is the unique condition of this family, which is transparent for all plane harmonic P and S waves striking the boundary Γ at normal incidence.*

We remark that the first-order condition ((1.1), (1.2)) depends on the geometry of the domain Ω since M depends on the unit exterior normal n.

In particular this condition becomes:

(1) In the case of a vertical boundary $(x_1 = 0)$

$$\begin{bmatrix} \sigma_{11} \\ \sigma_{21} \end{bmatrix} + \rho \begin{pmatrix} V_P & 0 \\ 0 & V_s \end{pmatrix} \begin{bmatrix} \dfrac{\partial u_1}{\partial t} \\ \dfrac{\partial u_2}{\partial t} \end{bmatrix} = 0;$$

(2) In the case of a horizontal boundary ($x_2 = 0$)

$$\begin{bmatrix} \sigma_{12} \\ \sigma_{22} \end{bmatrix} + \rho \begin{pmatrix} V_S & 0 \\ 0 & V_P \end{pmatrix} \begin{bmatrix} \dfrac{\partial u_1}{\partial t} \\ \dfrac{\partial u_2}{\partial t} \end{bmatrix} = 0.$$

Classically, the first-order condition ((1.1), (1.2)) is analyzed in terms of reflection of a plane harmonic P or S wave, with amplitude 1, striking the absorbing boundary Γ with an incidence θ, $0 \le \theta \le \pi/2$. We can show the following for a given θ:

(1) An incident P wave gives rise to a reflected P wave with amplitude $R_{PP}(\theta, \nu)$ and to a reflected S wave of amplitude $R_{PS}(\theta, \nu)$.

(2) An incident S wave gives rise to a reflected S wave with amplitude $R_{SS}(\theta, \nu)$ and to a reflected P wave of amplitude $R_{SP}(\theta, \nu)$.

The coefficients $R_{PP}(\theta, \nu)$ $R_{PS}(\theta, \nu)$ (respectively, $R_{SS}(\theta, \nu)$, $R_{SP}(\theta, \nu)$) are by definition the reflection coefficients of a P wave (respectively, of an S wave) for the absorbing boundary Γ. They depend on only the angle of incidence θ and the Poisson coefficient ν.

In particular we can show that for small angles of incidence θ,

$$R_{PP}(\theta, \nu) = O(\theta^2), \qquad R_{PS}(\theta, \nu) = O(\theta),$$

$$R_{SS}(\theta, \nu) = O(\theta^2), \qquad R_{SP}(\theta, \nu) = O(\theta),$$

which show that the first-order condition is "quasi-transparent" for small values of θ, the results in each case being better for the phenomena of pure reflection ($P \to P$, $S \to S$) than for the phenomena of conversion ($P \to S$, $S \to P$).

1.2. The reflection of Rayleigh waves. Now we consider the numerical simulation of the propagation of elastic waves in a homogeneous half space, $x_2 \le 0$, with the free surface boundary condition on the boundary $\Gamma_1(x_2 = 0)$,

(1.4) $$\begin{bmatrix} \sigma_{12} \\ \sigma_{22} \end{bmatrix} = 0 \quad \text{on } \Gamma_1.$$

It is well known that in such a medium, besides the so-called "volume waves," i.e., P and S waves, there also propagate surface waves guided by the free boundary Γ_1. These are the Rayleigh waves, which are the solutions of the form

(1.5) $$u_R(x_1, x_2, t) = U_R(x_1 \pm V_R t, x_2),$$

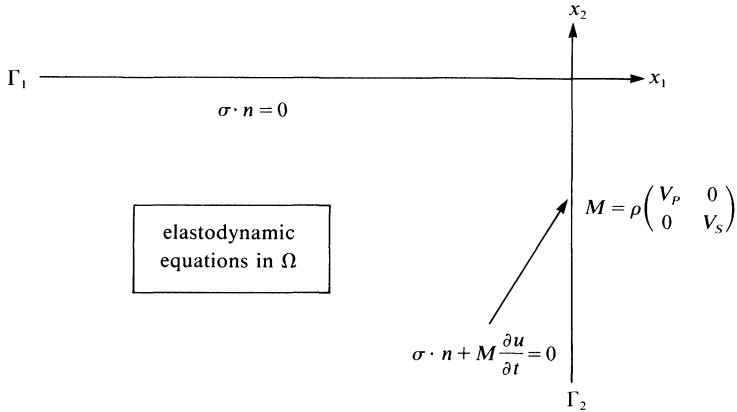where $C = V_R$ is the unique solution in the interval $[0, V_S]$ of the classical Rayleigh equation

(1.6) $$4\left(1 - \frac{C^2}{V_P^2}\right)^{1/2}\left(1 - \frac{C^2}{V_S^2}\right)^{1/2} = \left(2 - \frac{C^2}{V_S^2}\right)^2.$$

For the present, we shall limit our domain of calculation to the quarter plane

$$\Omega = \{(x_1, x_2) \in \mathbb{R}^2 : x_1 \le 0, x_2 \le 0\},$$

and take for boundary condition on the artificial boundary $\Gamma_2(x_1 = 0)$ the first-order absorbing boundary condition

(1.7) $$\begin{bmatrix} \sigma_{11} \\ \sigma_{21} \end{bmatrix} + \rho \begin{bmatrix} V_P & 0 \\ 0 & V_S \end{bmatrix} \begin{bmatrix} \dfrac{\partial u_1}{\partial t} \\ \dfrac{\partial u_2}{\partial t} \end{bmatrix} = 0 \quad \text{on } \Gamma_1.$$

x_2

Γ_1 ——————————————————→ x_1

$\sigma \cdot n = 0$

$M = \rho \begin{pmatrix} V_P & 0 \\ 0 & V_S \end{pmatrix}$

elastodynamic
equations in Ω

$\sigma \cdot n + M \dfrac{\partial u}{\partial t} = 0$

Γ_2

We can easily verify that a Rayleigh wave propagating along the free boundary Γ_1 in the positive x_1 direction, i.e., a wave incident upon the artificial boundary Γ_2,

(1.8) $u(x_1, x_2, t) = U_R(x_1 - V_R t, x_2),$

does not satisfy condition (1.7). In other words, the first-order condition is not transparent for Rayleigh waves.

Thus, the question that naturally arises is the following: What happens when a Rayleigh wave reaches the absorbing boundary Γ_2? The mathematical analysis of the phenomenon is extremely difficult. Only a numerical simulation permits us to have, in a simple manner, an idea of what happens—at least qualitatively.

1.3. Numerical results with the first-order absorbing boundary conditions. The results we shall present now were obtained by limiting the domain of calculation to a rectangle Ω. One of the sides of the rectangle coincides with the free boundary Γ_1. The other three sides are absorbing; we have taken the first-order condition on these sides. The rectangle has width 168 meters and depth 96 meters.

x_2

free boundary

x_1

S

Ω

$V_P = 1500 \text{ m/s}$

$V_S = 750 \text{ m/s}$

absorbing boundary
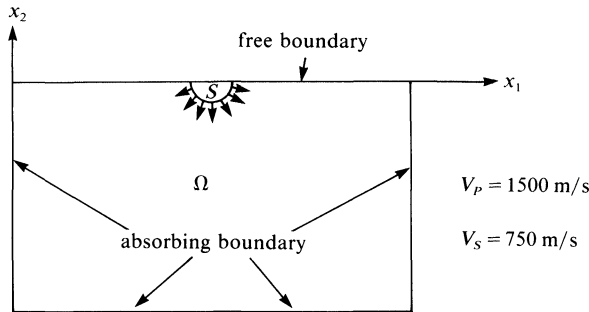
The elastic waves are excited by the explosion, at time $t = 0$, of a seismic source centered at point S on the free surface. The following results were obtained by a numerical simulation in which $Q1$ finite elements associated with a uniform grid were used for the spatial discretization, and an explicit scheme was employed for the time discretization. The meshsize was taken to be $\Delta x = 1$ m and the timestep $\Delta t = 0.5$ ms.

Figures 1.1–1.5 represent "snapshots" of the elastic medium Ω at different instants. Each figure presents, at a given time, an image of the deformed medium, in that each point of the grid has been displaced by its (amplified) displacement vector u. Thus the compressed regions are darker and the dilated regions lighter.
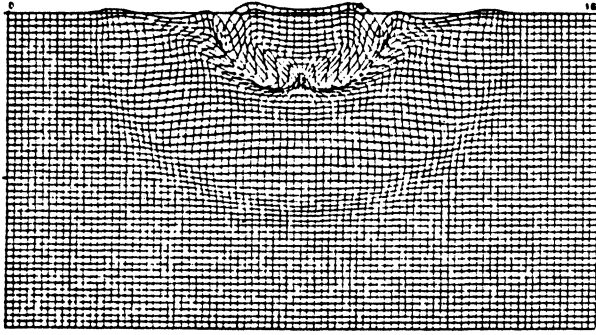
FIG. 1.1. *Deformed grid. Date*: 40 *milliseconds. Amplification Factor* (AF) = 3. *One trace every* 2 *meters.*
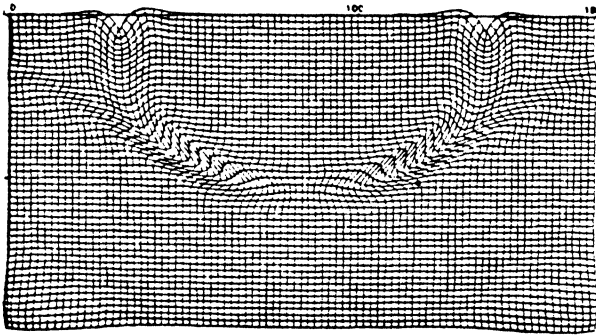

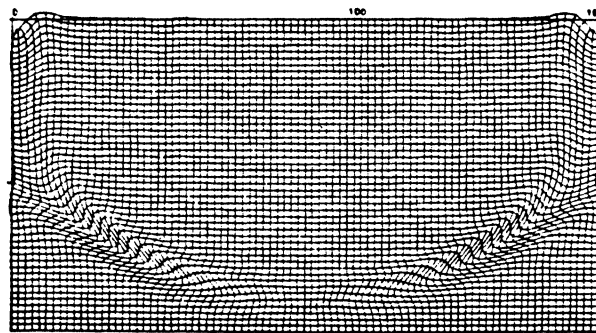FIG. 1.2. *Deformed grid. Date*: 80 *milliseconds.* AF = 3. *One trace every* 2 *meters.*

FIG. 1.3. *Deformed grid. Date*: 120 *milliseconds.* AF = 3. *One trace every* 2 *meters.*
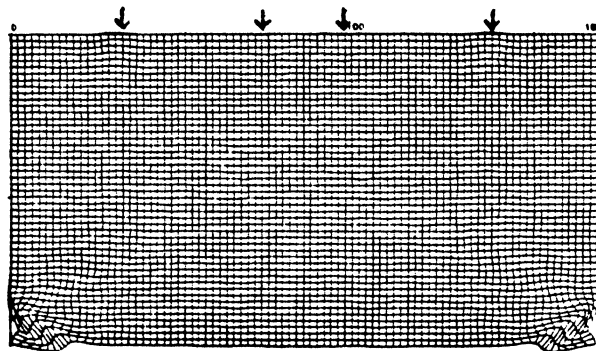

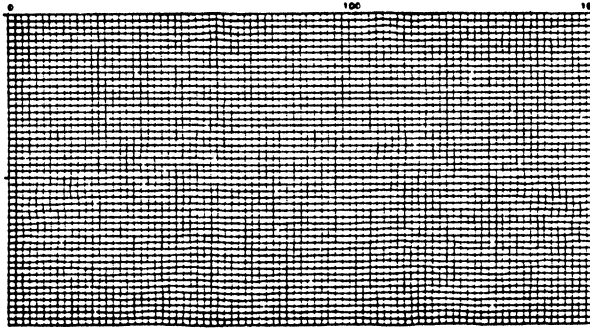FIG. 1.4. *Deformed grid. Date*: 160 *milliseconds.* AF = 3. *One trace every* 2 *meters.*
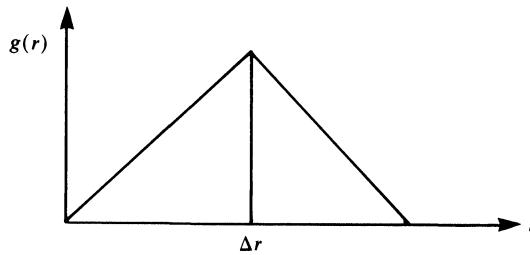
FIG. 1.5. *Deformed grid. Date: 200 milliseconds. AF = 3. One trace every 2 meters.*

The source was placed at the surface in order to generate surface waves with a large amplitude. We consider a source of compressional waves. The source is modeled by a right-hand side of the form

$$f(x, t) = g(\|x - s\|)h(t)\frac{x - s}{\|x - s\|},$$

where $g(r)$ is of the following form:

and $h(t)$ is a first-order Ricker, i.e., the first derivative of a Gaussian, with frequency centered at 80 hz.

The P wave front we see only in Fig. 1.1. The second circular front is due to the conversion at the free surface of the P wave to an S wave. This shear wave is joined to the P wave front by the head wave and to the Rayleigh wave, which corresponds to the large perturbation that disturbs the free surface as it propagates along it.

In Figs. 1.1 and 1.2, the Rayleigh wave has not yet reached the absorbing boundary. On the other hand, we can see that the P and S waves cross the artificial boundary without being noticeably reflected. The Rayleigh wave reaches the vertical boundary in Fig. 1.3, and in Figs. 1.4 and 1.5 we see that it has suffered a parasitic reflection. We can observe, propagating along the surface, two fronts converging toward the source, one with velocity V_P and the other with velocity V_R. While these parasitic waves might appear to be negligible, in fact they are not at all: The waves are of the same order of magnitude as the quantities actually measured in the seismic reflection experiments, which are themselves due to the reflection of the emitted wave by the heterogeneities of the substratum.

A finer analysis of these phenomena can be carried out by the examination of the synthetic seismograms, which, placed one next to the other, are the diagrams depicting the curves that give the variations of the two components, vertical and horizontal, of the displacements of the points of the free surface as functions of time. As the amplitude of volume waves decreases with time, we have amplified the results linearly in time in

order to better observe these waves at later times; see Figs. 1.6 and 1.7. (The amplitude of the Rayleigh waves, which do not decay in time, of course, appears to increase.)

We can clearly distinguish two lines D_p and D_R with respective slopes $1/V_p$ and $1/V_R$, which correspond to the propagation of the P wave and the Rayleigh wave. Equally well we see lines, D_{RP} and D_{RR}, issuing from the point of intersection of the line D_R with the curve corresponding to the right extremity of the model. These lines have slopes $-1/V_p$ and $-1/V_R$, respectively.

The line D_{RR} with slope $-1/V_R$ corresponds to the Rayleigh wave reflected by the absorbing boundary. When it arrives at the vertical boundary, the incident Rayleigh wave also gives rise to a compression wave that seems to be emitted by the corner point where the free and artificial boundaries intersect. It is this wave that explains the presence of the line D_{RP} with slope $-1/V_P$. This is a phenomenon of conversion from a surface wave to a volume wave. These two lines correspond, of course, to the parasitic fronts observed in Fig. 1.4.
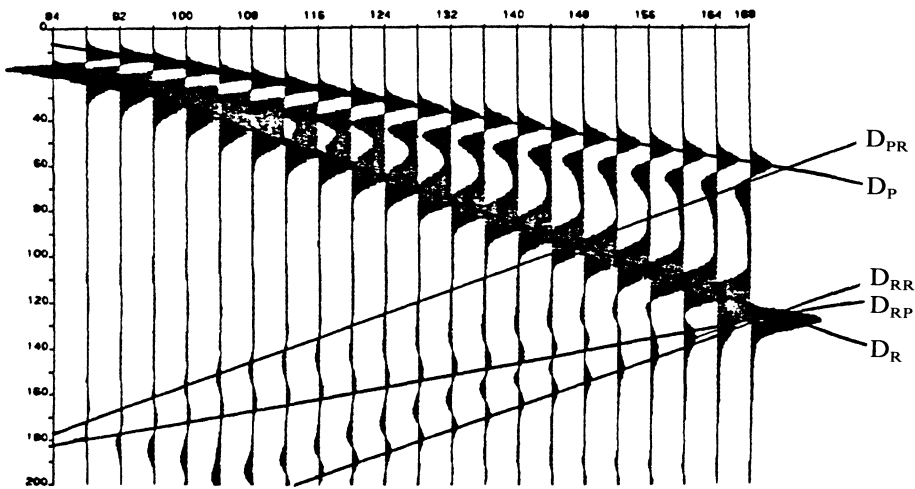
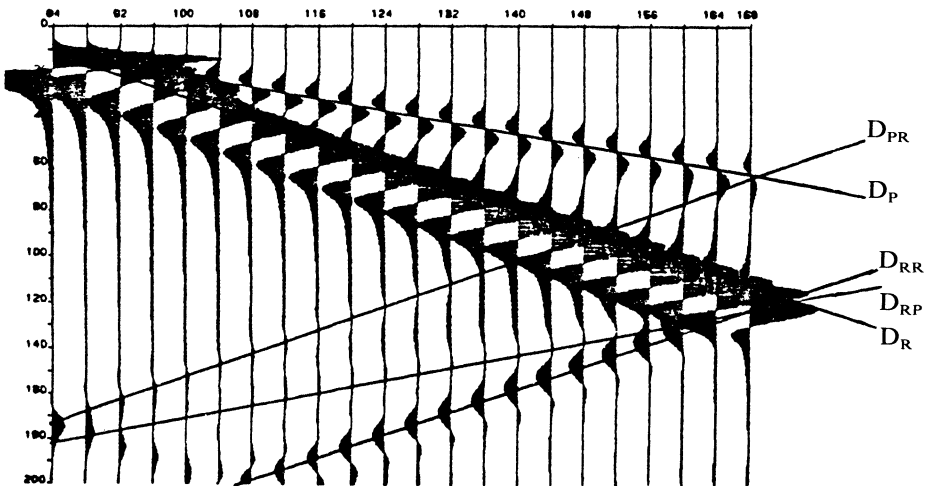FIG. 1.6. *Horizontal displacement. Gradient of amplification* $= 1 \times 10^{-4}$.

FIG. 1.7. *Vertical displacement. Gradient of amplification* $= 1 \times 10^{-4}$.

There appears yet another line D_{PR}, a second line of slope $-1/V_R$, that intersects the rightmost seismogram, the one corresponding to the registration at the upper right-hand corner of the model, at the same point as does the line D_P representing the incident P wave: this P wave, arriving at the vertical boundary, generates a parasitic Rayleigh wave. Anyway, this wave has a very small amplitude, even when compared with that of the reflected Rayleigh wave represented by the line D_{RR}, and is visible in Figs. 1.6 and 1.7 only for large values of t, i.e., when the amplification factor is maximum. This is a phenomenon of conversion of a volume wave to a surface wave. This is not in contradiction with the fact that the first-order absorbing condition is transparent for normally incident P waves, as here we have, in fact, the presence of a corner joining a free boundary with an absorbing boundary, a condition that we do not know how to analyze mathematically.

2. A first solution of geometric type: ears.

2.1. Description of the geometric solution. In the previous section we have seen that though the first-order absorbing boundary condition is transparent for normally incident P and S waves, when this boundary condition is used for an artificial boundary in the problem of a half space with free boundary, we still have the problem of reflected and converted surface waves. There are two evident ways to approach this problem. The first, and more rudimentary, is to try to modify the geometry of the domain of calculation to avoid having the corner connecting the free boundary with the absorbing boundary. The second is to modify the boundary condition itself. It is the first of these that we shall consider in this paragraph.

Since the amplitude of Rayleigh waves decreases exponentially with the distance from the free boundary, a very simple solution to the problem of the reflection of such waves at an artificial boundary is to enlarge the domain of calculation in a small region around the free boundary. In this way the length of time necessary for a Rayleigh wave to reach the artificial boundary and to be reflected back into the domain of interest can be made larger than the length of time of observation so that no reflection of a Rayleigh wave is detected.

Thus, if we consider the example of the previous paragraph, the idea is to modify our rectangular domain of calculation by adding to it two long thin rectangles (ears) in such a way as to extend the length of the free boundary on both sides of the original domain. More precisely, if we assume that our free boundary coincides with the axis $x_2 = 0$ and that our original domain was the rectangle $\Omega_1 = [0, 2l] \times [0, -d]$ with source S at $(l, 0)$, then our enlarged domain would be

$$\Omega_2 = \Omega_1 \cup E_l \cup E_r,$$

where we have set (with $b < d$)

$$E_l = [-a, 0] \times [0, -b], \qquad E_r = [2l, 2l+a] \times [0, -b].$$
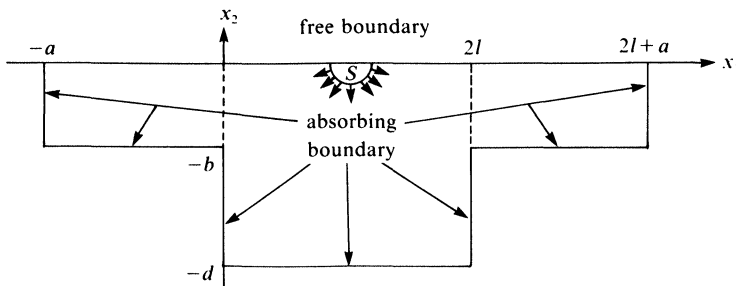
The constant a should be chosen large enough so that the time, $(l+a)/V_R + a/V_P$, needed for a Rayleigh wave to travel the distance $l+a$ and for the converted P wave to return the distance a to the domain of observation exceeds T, where T represents the final time of the observation. The depth b should be just of sufficient size for the amplitude of a Rayleigh wave to be negligible at that distance from the free boundary, but not so large as to greatly increase the time of calculation.

2.2. Numerical results for the geometric solution. The following figures represent the results of the same experiment as do those presented in paragraph 1.3, except that the domain of calculation here is Ω_2 instead of Ω_1. As before, Ω_1 is a rectangle of width 168 meters and depth 96 meters, and the source is centered at depth 0. At the midpoint of the upper edge of Ω_1, the depth of the ears is 49 meters. To reduce the number of our calculations, we have taken Ω to be only roughly twice the depth of the ears, whereas in practice the depth of Ω_1 would be much greater.
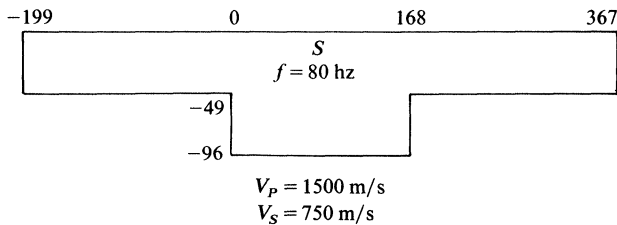
Figures 2.1–2.4 are the snapshots corresponding to those of Figs. 1.1–1.4. Figures 2.1 and 1.1 are, of course, identical, as the disturbance has not yet reached the artificial
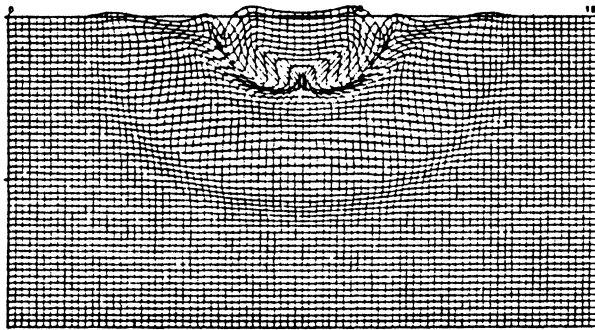
FIG. 2.1. *Deformed grid. Date*: 40 *milliseconds. Amplification Factor* (AF) = 3. *One trace every* 2 *meters.*
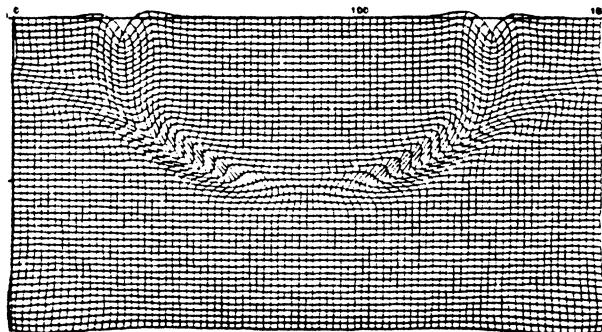
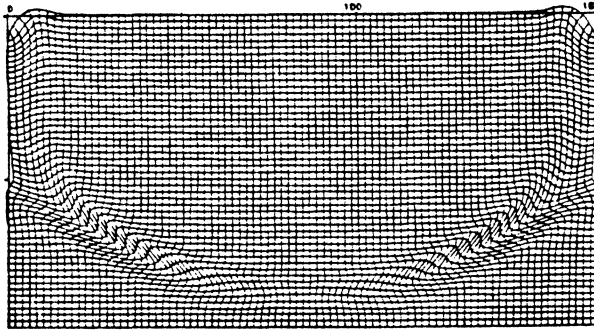FIG. 2.2. *Deformed grid. Date*: 80 *milliseconds.* AF = 3. *One trace every* 2 *meters.*

FIG. 2.3. *Deformed grid. Date: 120 milliseconds. AF = 3. One trace every 2 meters.*
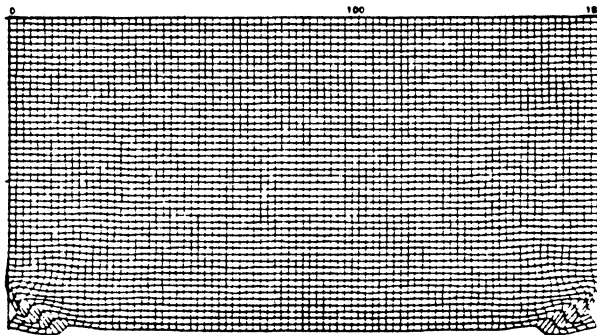

FIG. 2.4. *Deformed grid. Date: 160 milliseconds. AF = 3. One trace every 2 meters.*

boundary. However, the fact that Figs. 2.2 and 1.2, as well as Figs. 2.3 and 1.3, appear indistinguishable indicates that the P and the S wave fronts have passed the interior corners, located at $(0, b)$ and $(2l, b)$ without any noticeable diffraction. In Fig. 2.3 the Rayleigh wave reaches the bounds of the observed domain and in Fig. 2.4 we see that it has passed into the ears without giving rise to the parasitic P wave or Rayleigh wave observed in Fig. 1.4.

In Figs. 2.5–2.7 we restrict our attention to roughly the right quarter of the observed domain as well as to the right ear itself. The times of observation are the same as those
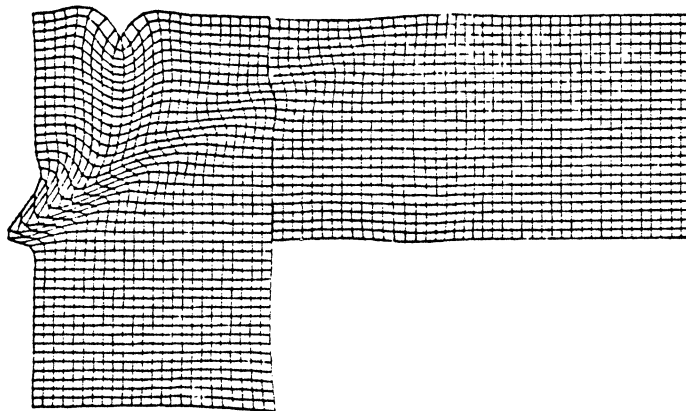

FIG. 2.5. *Deformed grid. Date: 80 milliseconds. AF = 3. One trace every 2 meters.*
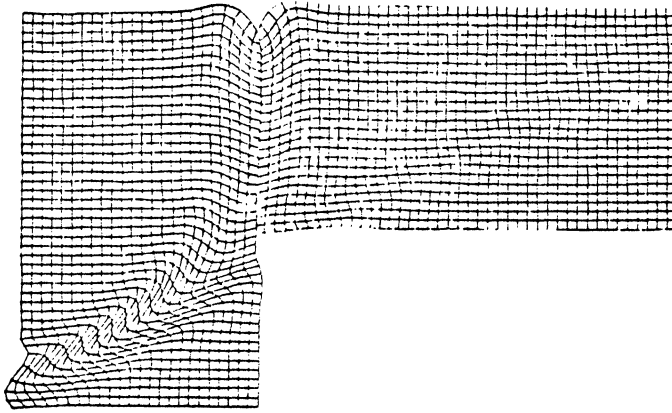
FIG. 2.6. *Deformed grid. Date*: 120 *milliseconds.* AF = 3. *One trace every* 2 *meters.*
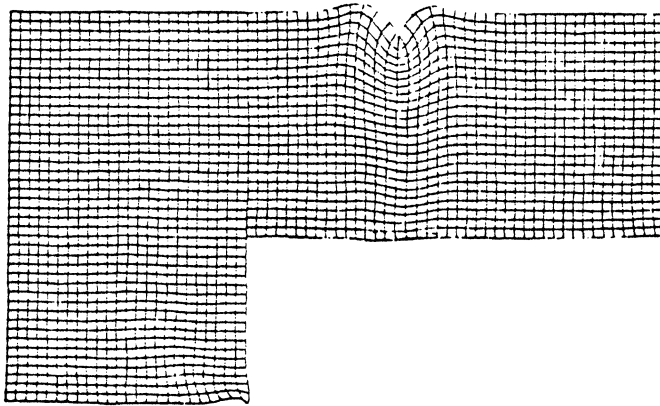

FIG. 2.7. *Deformed grid. Date*: 160 *milliseconds.* AF = 3. *One trace every* 2 *meters.*

in Figs. 1.2, 1.3, and 1.4, respectively, as well as in Figs. 2.2, 2.3, and 2.4. In Figs. 2.5, 2.6, and 2.7, we see the Rayleigh wave and S wave as they propagate toward the artificial boundary, reach the right ear, and move into the ear with apparently no problem. However, to more closely observe what happens at the interior corner, we look again at Fig. 2.8 at the deformation seen in Fig. 2.7, but this time with an amplification factor 10 times larger. In Fig. 2.8 a diffraction due to the corner is definitely visible, though it is not immediately evident if this is due to the S wave, the Rayleigh wave, or even the connecting wave between the two.

The seismograms corresponding to those presented in Figs. 1.6 and 1.7 are given in Figs. 2.9 and 2.10. As in Figs. 1.6 and 1.7, we can clearly distinguish the two lines D_p and D_R, having slopes $1/V_p$ and $1/V_R$, respectively, resulting from the disturbance caused by the P wave and Rayleigh wave arising at the source. However, the lines D_{RR} and D_{RP}, which correspond to the reflected and converted Rayleigh wave as well as the line D_{PR}, which corresponds to the conversion of the incident P wave to a parasitic Rayleigh wave, have disappeared. Thus, even for the large amplication factors toward the final time, there is no trace of these parasitic waves since the boundary giving rise to them has been pushed farther from the source.
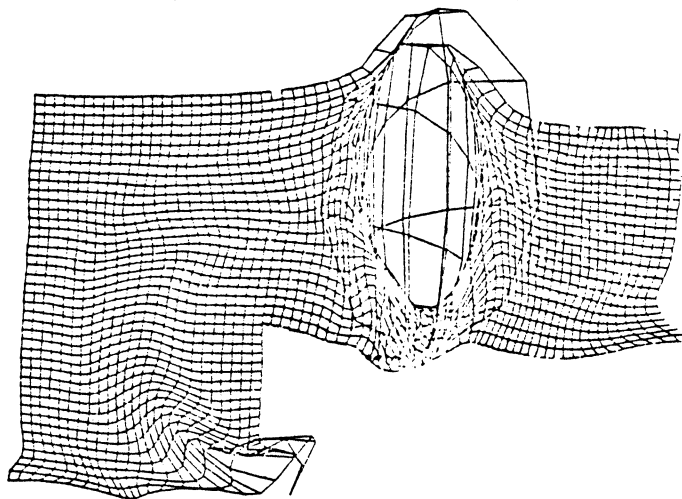
FIG. 2.8. *Deformed grid. Date*: 160 *milliseconds.* AF = 30. *One trace every* 2 *meters.*
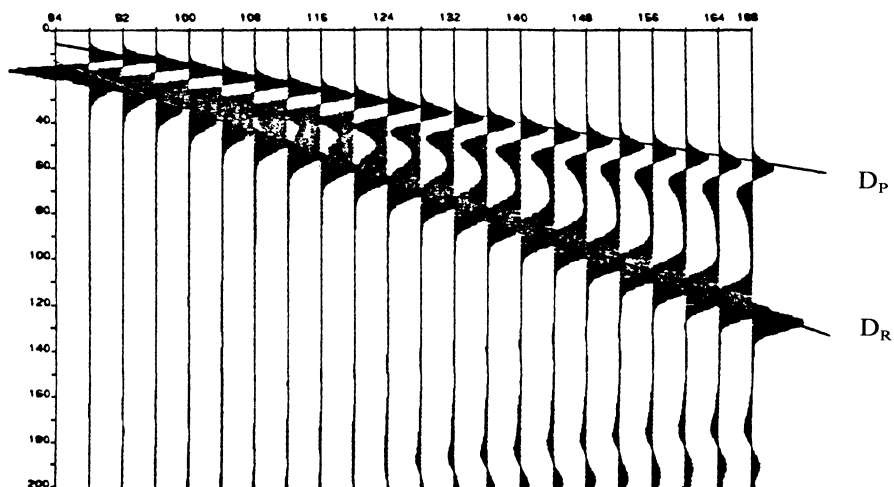

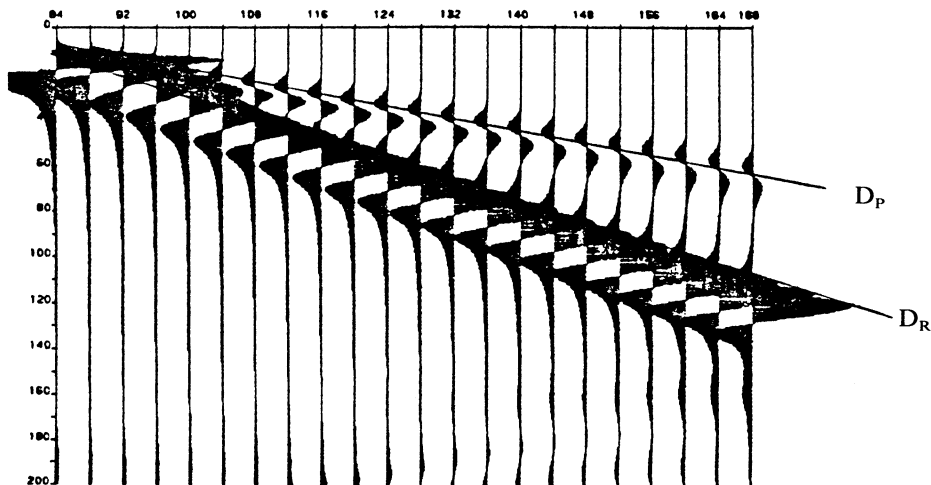FIG. 2.9. *Horizontal displacement. Gradient of amplification* = 1×10^{-4}.

FIG. 2.10. *Vertical displacement. Gradient of amplification* = 1×10^{-4}.

However, in Fig. 2.9, representing horizontal displacement, and to a lesser extent in Fig. 2.10, representing vertical displacement, there is a definite disturbance indicated in the lower right-hand corner. This perturbation corresponds to the phenomenon already detected in Fig. 2.8, which is due to the diffraction at the interior corner.

To further examine the phenomenon of diffraction at the interior corner, we have repeated the previous experiment, increasing the depth of the original rectangle to 192 meters and that of the ears to 99 meters, and also increasing the final time of the observation from 200 milliseconds to 400 milliseconds.
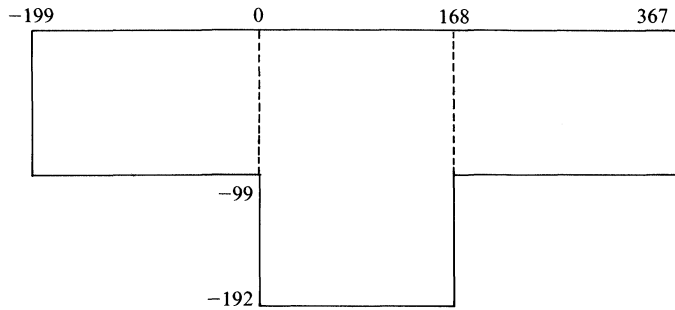
Figures 2.11 and 2.12 are snapshots at 200 milliseconds and 220 milliseconds, respectively. In both we still observe the diffraction phenomenon. Figure 2.13 represents the corresponding seismogram, depicting horizontal displacement. At around 275 milliseconds, there appears the same sort of disturbance as seen in Fig. 2.8, only here at a later time, because the corner is farther from the source. We remark that an analysis of the velocity indicates that the nature of the diffracted disturbance is probably an S wave; and again we emphasize that the amplification factor in the seismograms at later times is quite large.

2.3. Conclusion. The ears solution is effective in eliminating the reflection and conversion of the Rayleigh wave at the artificial absorbing boundary. It also eliminates the parasitic Rayleigh wave generated when the incident P wave reaches the corner joining the free boundary with the artificial boundary. However, the interior corners introduced by the addition of the ears do give rise to a diffraction that, though smaller in amplitude than the parasitic Rayleigh waves, is still of an order that can be detected
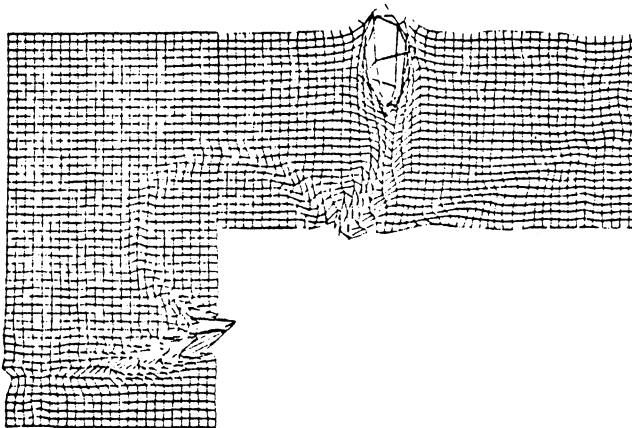
FIG. 2.11. *Deformed grid. Date: 200 milliseconds. AF = 20. One trace every 4 meters.*
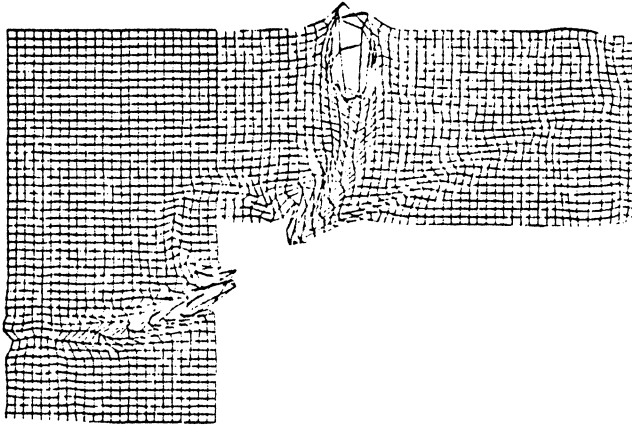
FIG. 2.12. *Deformed grid. Date*: 220 *milliseconds.* AF = 20. *One trace every* 4 *meters.*
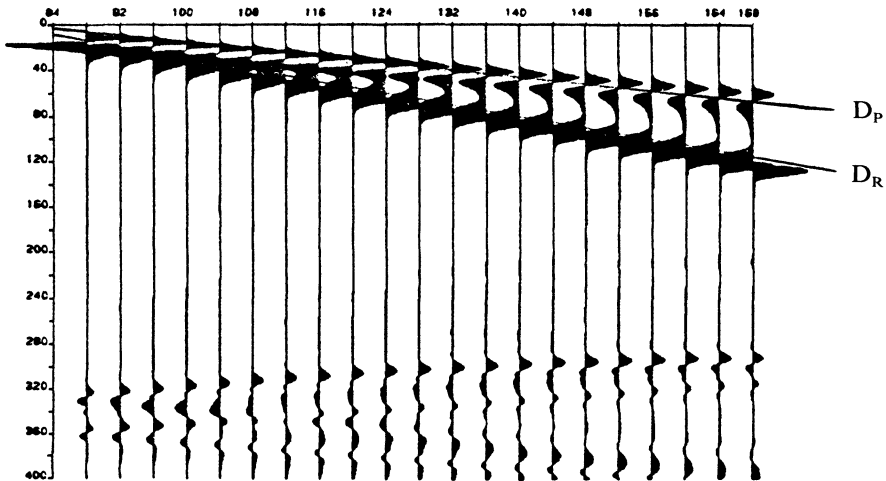
FIG. 2.13. *Horizontal displacement. Gradient of amplification* = 1×10^{-4}.

in the snapshots and seismograms. We can hope to improve these results by modifying the absorbing condition in a neighborhood of the corner.

Finally, we should note that though the addition of the ears should not significantly increase the time of calculation, it does complicate the programming. Still this complication is not extraordinary, as the ears may be programmed once and for all, independent of the complexity of the model.

3. A condition transparent for *P*, *S*, and *R* waves.

3.1. Derivation and analysis of a new condition. We restrict our attention to the case of a half plane Ω with boundary, the line Γ having unit normal vector n. The first-order condition

$$\mathscr{L}_1(u) = \sigma \cdot n + M \frac{\partial u}{\partial t} = 0,$$

with M the symmetric positive definite matrix

$$M = \begin{pmatrix} n_1 & n_2 \\ n_2 & -n_1 \end{pmatrix} \begin{pmatrix} \rho V_P & 0 \\ 0 & \rho V_S \end{pmatrix} \begin{pmatrix} n_1 & n_2 \\ n_2 & -n_1 \end{pmatrix},$$

is transparent for all P and S waves with normal incidence. Let us now consider the differential operator

$$\frac{\partial}{\partial t} + Cn \cdot \text{grad},$$

where C designates a positive velocity. Clearly we have

$$\frac{\partial u}{\partial t} + Cn \cdot \text{grad } u = 0$$

for any C wave with normal incidence, i.e., for any wave u of the form

$$u(x, t) = u_C(x \cdot \tau, x \cdot n - Ct),$$

where τ is a unit vector tangent to Γ, and u_C is an arbitrary vectorial function of two scalar variables. We introduce the operator

$$\mathscr{L}_C(u) = \left(\frac{\partial}{\partial t} + Cn \cdot \text{grad} \right) \mathscr{L}_1(u)$$

and the boundary condition

(3.1) $\mathscr{L}_C(u) = 0$ on Γ.

We remark that this condition is:
    (1) In the case of a left half plane with Γ a vertical boundary

$$\left(\frac{\partial}{\partial t} + C \frac{\partial}{\partial x_1} \right) \mathscr{L}_1(u) = 0 \quad \text{on } \Gamma,$$

with

$$\mathscr{L}_1(u) = \begin{bmatrix} \sigma_{11} \\ \sigma_{21} \end{bmatrix} + \rho \begin{pmatrix} V_p & 0 \\ 0 & V_S \end{pmatrix} \begin{bmatrix} \dfrac{\partial u_1}{\partial t} \\ \dfrac{\partial u_2}{\partial t} \end{bmatrix};$$

    (2) In the case of a lower half plane with Γ a horizontal boundary

$$\left(\frac{\partial}{\partial t} + C \frac{\partial}{\partial x_2} \right) \mathscr{L}_1(u) = 0 \quad \text{on } \Gamma,$$

with

$$\mathscr{L}_1(u) = \begin{bmatrix} \sigma_{12} \\ \sigma_{22} \end{bmatrix} + \rho \begin{pmatrix} V_S & 0 \\ 0 & V_P \end{pmatrix} \begin{bmatrix} \dfrac{\partial u_1}{\partial t} \\ \dfrac{\partial u_2}{\partial t} \end{bmatrix}.$$

THEOREM 3.1. *The boundary condition* (3.1) *is transparent for the following*:
    (i) *P waves at normal incidence*;
    (ii) *S waves at normal incidence*;
    (iii) *C waves at normal incidence*.

Proof. The first two points are clear. The last is also clear together with the observation that $\mathcal{L}_C(u)$ may also be written in the form

$$\mathcal{L}_C(u) = \mathcal{L}_1\left(\frac{\partial u}{\partial t} + Cn \cdot \operatorname{grad} u\right).$$

The operator $\partial/\partial t + Cn \cdot \operatorname{grad}$ is diagonal, and thus, as C is constant, commutes with $\mathcal{L}_1$. □

We turn now to the question of the stability of (3.1). For simplicity of exposition, we consider the case Ω the left half plane,

$$\Omega = \{(x_1, x_2)\,|\,x_1 < 0\}, \qquad \Gamma = \{(x_1, x_2)\,|\,x_1 = 0\}.$$

Then the problem may be written as follows:

$$\rho\frac{\partial^2 u_1}{\partial t^2} = \frac{\partial}{\partial x_1}\sigma_{11} + \frac{\partial}{\partial x_2}\sigma_{12}$$

$$\rho\frac{\partial^2 u_2}{\partial t^2} = \frac{\partial}{\partial x_1}\sigma_{21} + \frac{\partial}{\partial x_2}\sigma_{22}$$

in Ω,

with boundary condition

(3.2) $$\mathcal{L}_C(u) = 0 \qquad\qquad \text{on } \Gamma$$

and with initial conditions

$$u(x, 0) = u^0(x)$$

$$\frac{\partial u}{\partial t}(x, 0) = \dot{u}^0(x)$$

in Ω.

THEOREM 3.2. *The problem (3.2) is well posed.*
Proof. We introduce the function w,

$$w = \frac{\partial u}{\partial t} + C\frac{\partial u}{\partial x_1}.$$

As u satisfies the equations of elastodynamics in Ω, so does w. Also w satisfies the initial conditions

$$w(x, 0) = w^0(x) = \dot{u}^0(x) + C\frac{\partial u^0}{\partial x_1}(x)$$

$$\frac{\partial w}{\partial t}(x, 0) = \dot{w}^0(x) = \frac{\partial^2 u}{\partial t^2}(x, 0) + C\frac{\partial^2 u}{\partial t\partial x_1}(x, 0)$$

in Ω.

An expression for $\partial^2 u/\partial t^2(x, 0)$ may be deduced from the equations satisfied by u at the initial time $t = 0$. Furthermore, the function w satisfies the boundary condition

$$\mathcal{L}_1(w) = 0, \quad \text{on } \Gamma.$$

We know (cf. § 1) that we can obtain energy estimations for w. Namely,

$$\int \left|\frac{\partial w}{\partial t}\right|^2 dx \leqq C(\|w^0\|^2 + \|\nabla w^0\|^2),$$

$$\int |\nabla w|^2 dx \leqq C(\|w^0\|^2 + \|\nabla w^0\|^2),$$

which easily lead to

$$\int_\Omega \left|\frac{\partial w}{\partial t}\right|^2 dx \leq C(\|u^0\|_{H^2}^2 + \|\dot{u}^0\|_{H^1}^2),$$

$$\int_\Omega |\nabla w|^2 dx \leq C(\|u^0\|_{H^2}^2 + \|\dot{u}^0\|_{H_1}^2).$$

Then, thanks to Gronwall's lemma

$$\forall t \leq T \quad \int |w|^2 dx \leq C(T)(\|u^0\|_{H^2}^2 + \|\dot{u}_1^0\|_{H^1}^2).$$

It remains to obtain estimates about u. For this we can use the following lemma.

LEMMA. *Let (v, ψ) satisfy in Ω the equation*

$$\frac{\partial v}{\partial t} + c\frac{\partial v}{\partial x_1} = \psi.$$

Then we have the following inequality, for any $t > 0$:

$$\left(\int_\Omega |v|^2 dx\right)^{1/2} \leq \int_0^t \left(\int_\Omega |\psi|^2 dx\right)^{1/2} ds + \left(\int_\Omega |v_0|^2 dx\right)^{1/2},$$

where $v_0(x) = v(x, 0)$.

Proof of the lemma. We multiply the equation by v and integrate over Ω, which gives

$$\frac{1}{2}\frac{d}{dt}\left(\int_\Omega |v|^2 dx\right) + \frac{c}{2}\int_{-\infty}^{+\infty} |v(0, x_2, t)|^2 dt = \int_\Omega \psi v \, dx,$$

from which we deduce

$$\frac{1}{2}\frac{d}{dt}\left(\int_\Omega |v|^2 dx\right) \leq \left(\int_\Omega |\psi|^2 dx\right)^{1/2}\left(\int_\Omega |v|^2 dx\right)^{1/2}.$$

Then Gronwall's lemma leads to the result. □
    We can now apply the previous lemma with

$$v = u, \qquad \psi = w,$$

$$v = \frac{\partial u}{\partial t}, \qquad \psi = \frac{\partial w}{\partial t},$$

$$v = \frac{\partial u}{\partial x_j}, \qquad \psi = \frac{\partial w}{\partial x_j}, \quad j = 1, 2,$$

which permits us to obtain the following: ($\forall t \in [0, T]$)

$$\int_\Omega |u|^2 dx \leq C(T)(\|u^0\|_{H^2}^2 + \|\dot{u}^0\|_{H^1}^2),$$

$$\int_\Omega \left|\frac{\partial u}{\partial t}\right|^2 dx \leq C(T)(\|u^0\|_{H^2}^2 + \|\dot{u}^0\|_{H^1}^2),$$

$$\int_\Omega |\nabla u|^2 dx \leq C(T)(\|u^0\|_{H^2}^2 + \|\dot{u}^0\|_{H^1}^2),$$

and the theorem follows. □

It is easy to check that in the operator $\mathscr{L}_C$, second derivatives in the normal direction to the boundary exist, which cause trouble.

The expression for the boundary condition (3.1) may be transformed in such a way that only first-order derivatives in the direction normal to Γ appear. In the expression for $\mathscr{L}_C(u)$,

$$\mathscr{L}_C(u) = \frac{\partial}{\partial t}(\sigma \cdot n) + Cn \cdot \text{grad}\,(\sigma \cdot n) + M\left(\frac{\partial^2 u}{\partial t^2} + C\frac{\partial}{\partial t}\,n \cdot \text{grad}\,u\right),$$

the term containing the second-order normal derivative is $Cn \cdot \text{grad}\,(\sigma \cdot n)$. Assuming that the equations of elastodynamics are satisfied on Γ, we deduce that

$$n \cdot \text{grad}\,(\sigma \cdot n) = -\tau \cdot \text{grad}\,(\sigma \cdot \tau) + \rho\frac{\partial^2 u}{\partial t^2},$$

where τ is a unit vector tangent to Γ.

Combining these two equations, we obtain

$$\frac{\partial}{\partial t}(\sigma \cdot n) - C\tau \cdot \text{grad}\,(\sigma \cdot \tau) + (M + \rho C1)\frac{\partial^2 u}{\partial t^2} + CM\frac{\partial}{\partial t}\,n \cdot \text{grad}\,u = 0.$$

Put

$$\tilde{\mathscr{L}}_C(u) = \frac{\partial}{\partial t}(\sigma \cdot n) - C(\tau)\,\text{grad}\,(\sigma \cdot \tau) + (M + \rho C1)\frac{\partial^2 u}{\partial t^2} + CM\frac{\partial}{\partial t}\,n \cdot \text{grad}\,u.$$

The operator $\tilde{\mathscr{L}}_C(u)$ may be written as follows:

(1) In the case of a left half plane with Γ a vertical boundary

$$\tilde{\mathscr{L}}_c(u) = \frac{\partial}{\partial t}\begin{bmatrix}\sigma_{11} \\ \sigma_{21}\end{bmatrix} - C\frac{\partial}{\partial x_2}\begin{bmatrix}\sigma_{12} \\ \sigma_{22}\end{bmatrix} + \rho\begin{pmatrix}V_P + C & 0 \\ 0 & V_S + C\end{pmatrix}\frac{\partial^2 u}{\partial t^2} + \rho C\begin{pmatrix}V_P & 0 \\ 0 & V_S\end{pmatrix}\frac{\partial^2 u}{\partial t\partial x_1};$$

(2) In the case of a lower half plane with Γ a horizontal boundary

$$\tilde{\mathscr{L}}_C(u) = \frac{\partial}{\partial t}\begin{bmatrix}\sigma_{12} \\ \sigma_{22}\end{bmatrix} - C\frac{\partial}{\partial x_1}\begin{bmatrix}\sigma_{11} \\ \sigma_{21}\end{bmatrix} + \rho\begin{pmatrix}V_S + C & 0 \\ 0 & V_P + C\end{pmatrix}\frac{\partial^2 u}{\partial t^2}$$

$$+ \rho C\begin{pmatrix}V_S & 0 \\ 0 & V_P\end{pmatrix}\frac{\partial^2 u}{\partial t\partial x_2}.$$
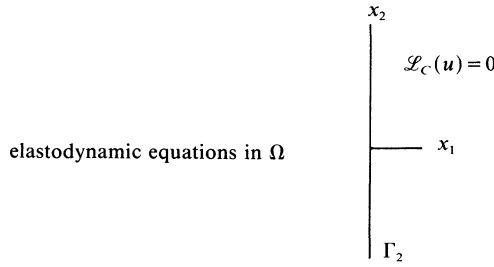
THEOREM 3.3. *The boundary condition* (3.1) *is equivalent to the condition*

$$\tilde{\mathscr{L}}_C(u) = 0.$$

3.2. Plane wave analysis. As in the case of the first-order condition, the condition (3.1) may be subjected to analysis in terms of the reflection coefficients R_{PP}, R_{PS}, R_{SS}, and R_{SP}, defined in § 1.2.

We take for domain Ω the left half plane $\{x\colon x_1 < 0\}$ and assume that on the boundary $\Gamma_2\{x\colon x_1 = 0\}$ we have the following absorbing boundary condition (3.1):

$$\mathscr{L}_C(u) = \left(\frac{\partial}{\partial t} + C\frac{\partial}{\partial x_1}\right)\mathscr{L}_1(u) = 0,$$

$$\mathscr{L}_1(u) = \begin{bmatrix}\sigma_{11} \\ \sigma_{21}\end{bmatrix} + \rho\begin{pmatrix}V_P & 0 \\ 0 & V_S\end{pmatrix}\frac{\partial u}{\partial t}.$$

x_2

$\mathscr{L}_C(u) = 0$

x_1

elastodynamic equations in Ω

Γ_2

Consider a harmonic P wave of unit norm,

$$u^P = u_P \, e^{i(k_P x - \omega t)},$$

propagating toward the boundary Γ_2. Suppose that upon arriving at Γ_2, u^P gives rise to a reflected P wave u^{PP} and a reflected S wave u^{PS}:

$$u^{PP} = R_{PP} u_{PP} \, e^{i(k_{PP} x - \omega t)} \qquad u^{PS} = R_{PS} u_{PS} \, e^{i(k_{PS} x - \omega t)}.$$

If the angle of incidence (measured from the normal) of u^P is θ, then the angle of emergence of u^{PP} is also θ and that of u^{PS} is ψ, where ψ is related to θ by Snell's law

$$\sin \psi = \frac{V_S}{V_P} \sin \theta.$$

We know that the length of the propagation vectors, k_P and k_{PP}, of the P waves is ω / V_P and that the length of k_{PS}, the propagation vector of the S wave, is ω / V_S.

Furthermore, the unit displacement vectors u_P and u_{PP} of the P waves are parallel to their propagation vectors k_P and k_{PP}, while the displacement vector u_{PS} for the S wave is perpendicular to k_{PS}:

$$k_P = \frac{\omega}{V_P} \begin{pmatrix} \cos \theta \\ \sin \theta \end{pmatrix}, \quad k_{PP} = \frac{\omega}{V_P} \begin{pmatrix} -\cos \theta \\ \sin \theta \end{pmatrix}, \quad k_{PS} = \frac{\omega}{V_S} \begin{pmatrix} -\cos \psi \\ \sin \psi \end{pmatrix},$$

$$u_P = \begin{pmatrix} \cos \theta \\ \sin \theta \end{pmatrix}, \quad u_{PP} = \begin{pmatrix} -\cos \theta \\ \sin \theta \end{pmatrix}, \quad u_{PS} = \begin{pmatrix} \sin \psi \\ \cos \psi \end{pmatrix}.$$

Now if we consider the sum u of these three waves,

$$u = u^P + R_{PP} u^{PP} + R_{PS} u^{PS},$$

we know that, by construction, u satisfies the equations of elastodynamics in Ω. By imposing that u also satisfy the condition (3.1), on Γ_2, we obtain the following linear system in the unknowns R_{PP} and R_{PS}:

(3.3)

$$(\cos \theta + 1)(2 \cos \theta + \kappa^2 - 2)(m \cos \theta + \kappa) R_{PP}$$
$$- \kappa^2 \sin \psi (2 \cos \psi + \kappa)(m \cos \psi + 1) R_{PS}$$
$$= (\cos \theta - 1)(2 \cos \theta - \kappa^2 + 2)(m \cos \theta - \kappa),$$

$$\sin \theta (2 \cos \theta + \kappa)(m \cos \theta + \kappa) R_{PP}$$
$$+ \kappa^2 (\cos \psi + 1)(2 \cos \psi - 1)(m \cos \psi + 1) R_{PS}$$
$$= -\sin \theta (2 \cos \theta - \kappa)(m \cos \theta - \kappa),$$

where κ is the ratio V_P / V_S given as a function of ν by

$$\kappa = \left(\frac{1(1 - \nu)}{1 - 2\nu} \right)^{1/2}$$

and m is the ratio C / V_S.

Similarly we obtain a system in the unknowns R_{SP} and R_{SS} by considering the reflection of a harmonic S wave of unit amplitude

$$u^S = u_S \, e^{i(k_S x - \omega t)}$$

by the boundary Γ_2. For an angle of incidence θ, there are a reflected P wave u^{SP} and a reflected S wave u^{SS}:

$$u^{SP} = R_{SP} u_{SP} \, e^{i(k_{SP} x - \omega t)}, \qquad u^{SS} = R_{SS} u_{SS} \, e^{i(k_{SS} x - \omega t)}$$

emerging at angles ψ and θ, respectively, with

(3.4) $$\sin \psi = \frac{V_P}{V_S} \sin \theta.$$

As before, the length of the propagation vector k_{SP} of the P wave is ω/V_P, while that of k_S and k_{SS} is ω/V_S, and the unit displacement vector u_{SP} is parallel to k_{SP}, while u_S and u_{SS} are orthogonal to k_S and k_{SS}, respectively:

$$k_S = \frac{\omega}{V_S} \begin{pmatrix} \cos \theta \\ \sin \theta \end{pmatrix}, \quad k_{SP} = \frac{\omega}{V_P} \begin{pmatrix} -\cos \psi \\ \sin \psi \end{pmatrix}, \quad k_{SS} = \frac{\omega}{V_S} \begin{pmatrix} -\cos \theta \\ \sin \theta \end{pmatrix},$$

$$u_S = \begin{pmatrix} -\sin \theta \\ \cos \theta \end{pmatrix}, \quad u_{SP} = \begin{pmatrix} -\cos \psi \\ \sin \psi \end{pmatrix}, \quad u_{SS} = \begin{pmatrix} \sin \theta \\ \cos \theta \end{pmatrix}.$$

Again, the linear system in R_{SP} and R_{SS} is obtained by requiring that the sum u of the incident wave u^S, with the two reflected waves $R_{SP} u^{SP}$ and $R_{SS} u^{SS}$, satisfy the boundary condition (3.1) on Γ_2. Thus, we have

$$(\cos \psi + 1)(2 \cos \psi + \kappa^2 - 2)(m \cos \psi + \kappa) R_{SP}$$

$$- \kappa^2 \sin \theta (2 \cos \theta + \kappa)(m \cos \theta + 1) R_{SS}$$

$$= -\kappa^2 \sin \theta (2 \cos \theta - \kappa)(m \cos \theta - 1),$$

(3.5)

$$\sin \psi (2 \cos \psi + \kappa)(m \cos \psi + \kappa) R_{SP}$$

$$+ \kappa^2 (\cos \theta + 1)(2 \cos \theta - 1)(m \cos \theta + 1) R_{SS}$$

$$= -\kappa^2 (\cos \theta - 1)(2 \cos \theta - 1)(m \cos \theta - 1).$$

We remark that (3.4) implies that for θ larger than arcsin $1/k$, $\sin \psi$ is larger than 1, i.e., ψ is no longer real. In this case, the propagation vector k_{SP} becomes

$$k_{SP} = \frac{\omega}{V_S} \begin{pmatrix} -i(\sin^2 \psi - 1)^{1/2} \\ \sin \psi \end{pmatrix}$$

and the reflected P wave

$$R_{SP} u^{SP} = R_{SP} u_{SP} \, e^{(\omega/V_S)(\sin^2 \psi - 1)^{1/2} x_1} \, e^{i(\omega/V_S)(\sin \psi x_2 - \omega t)}$$

is no longer a harmonic wave but is a surface wave propagating along the boundary Γ with amplitude decreasing exponentially with distance from Γ_2.

THEOREM 3.4. *The reflection coefficients* R_{PP}, R_{PS}, R_{SP}, *and* R_{SS} *depend only on the angle of incidence* θ, *the Poisson coefficient* ν, *and the ratio* C/V_S, *and for small angles of incidence* θ:

    (i) *For* $C = V_P$:

$$R_{PP}(\theta, \nu) = O(\theta^4), \qquad R_{PS}(\theta, \nu) = O(\theta^3),$$

$$R_{SS}(\theta, \nu) = O(\theta^2), \qquad R_{SP}(\theta, \nu) = O(\theta).$$

(ii) *For* $C = V_S$:

$$R_{PP}(\theta, \nu) = O(\theta^2), \qquad R_{PS}(\theta, \nu) = O(\theta),$$

$$R_{SS}(\theta, \nu) = O(\theta^4), \qquad R_{SP}(\theta, \nu) = O(\theta^3).$$

(iii) *For* $C \neq V_P$, $C \neq V_S$:

$$R_{PP}(\theta, \nu, C/V_S) = O(\theta^2), \qquad R_{PS}(\theta, \nu, C/V_S) = O(\theta),$$

$$R_{SS}(\theta, \nu, C/V_S) = O(\theta^2), \qquad R_{SP}(\theta, \nu, C/V_S) = O(\theta).$$

Proof. Using (3.3), we obtain by a direct calculation:

$$R_{PP} = \left[-\frac{(4-\kappa^2)(1+\kappa)m}{4\kappa^3(m+\kappa)} + O(\theta^2) \right]\left(1 - \frac{\kappa}{m} - \frac{\theta^2}{2} \right)\theta^2,$$

$$R_{PS} = \left[-\frac{(2-\kappa)m}{2\kappa^2(m+1)} + O(\theta^2) \right]\left(1 - \frac{\kappa}{m} - \frac{\theta^2}{2} \right)\theta.$$

Thus, for $C = V_P$, we have $m = \kappa$, and the term $(1 - \kappa/m - \theta^2/2)$ gives another factor of θ^2 in the expressions for R_{PP} and R_{PS}.

Similarly, from (3.5) we obtain

$$R_{SS} = \left[-\frac{(\kappa-4)(\kappa+1)m}{4\kappa(m+1)} + O(\theta^2) \right]\left(1 - \frac{1}{m} - \frac{\theta^2}{2} \right)\theta^2,$$

$$R_{SP} = \left[-\frac{(2-\kappa)m}{2(m+\kappa)} + O(\theta^2) \right]\left(1 - \frac{1}{m} - \frac{\theta^2}{2} \right)\theta,$$

and observe that for $C = V_S$, a factor of θ^2 is gained from the term $(1 - 1/m - \theta^2/2)$ in the expressions for R_{SS} and R_{SP}. $\square$

In Figs. 3.1 and 3.2 the amplitudes R_{PP}, R_{PS}, R_{SS}, and R_{SP} for the boundary conditions $\mathcal{L}_1(u) = 0$ and $\mathcal{L}_C(u) = 0$ with $C = V_P$ may be compared. These curves give the reflection coefficients for various values of the Poisson coefficient ν, from 0.0 to 0.48, as functions of the angle of incidence θ. We have not distinguished here the different values of ν: we want only to emphasize the weak influence of this parameter. We remark that even for the coefficients R_{SP} and R_{ss}, which are of the same order in θ for both conditions, the results seem to be better for the condition $\mathcal{L}_C(u) = 0$.

The corresponding curves for the condition $\mathcal{L}_C(u) = 0$ with $C = V_S$ and $C = V_R$ are shown in Fig. 3.2. We can easily see that, for all values of C we have considered, the various reflection coefficients have been uniformly improved (not only for small values of θ).

3.3. A condition transparent for P, S, and R waves. We return now to our example of the half space $x_2 < 0$ with free boundary $\Gamma_1, \Gamma_2 = 0$. We restrict our domain of calculation, as in § 1.2, to the quarter plane

$$\Omega = \{x: x_1 \leq 0 \text{ and } x_2 \leq 0\},$$

and take for boundary condition on the artificial boundary Γ_2, $x_1 = 0$ the condition (3.1), $\mathcal{L}_{V_R}(u) = 0$.
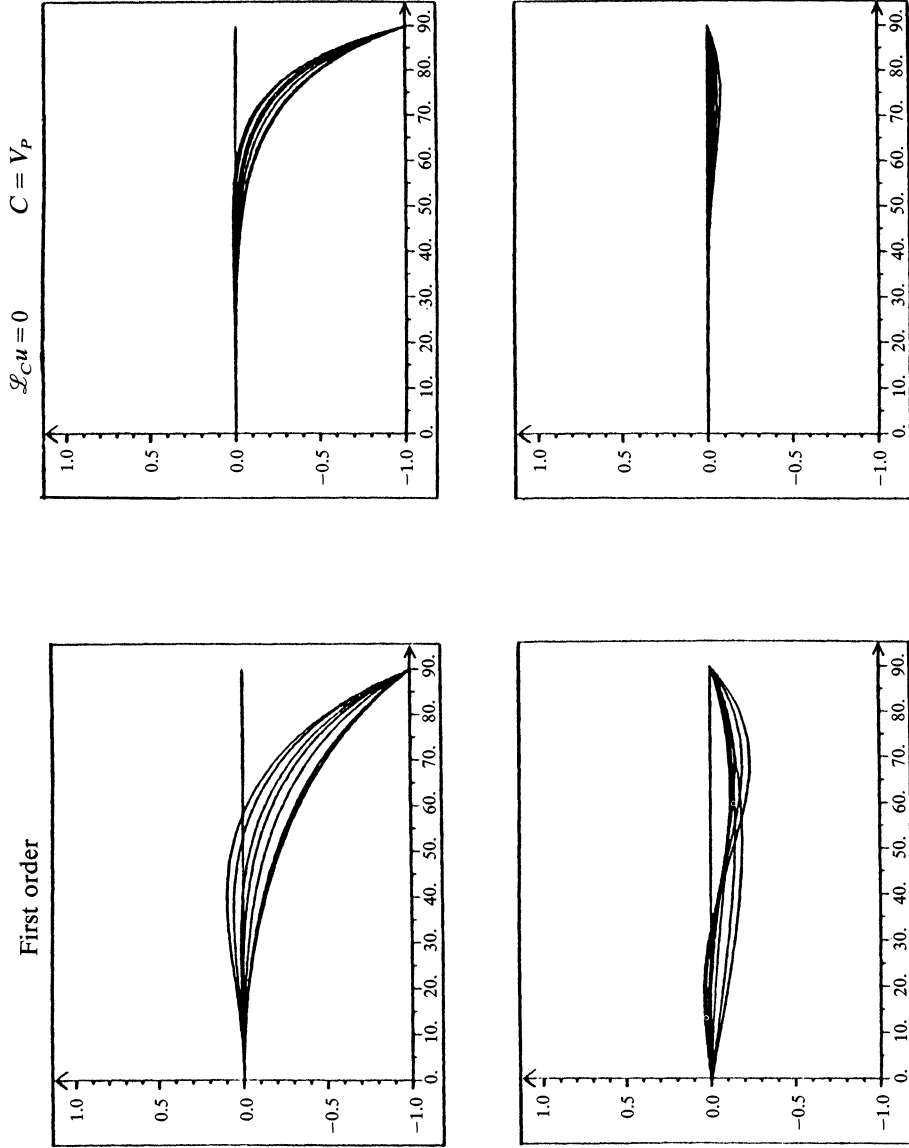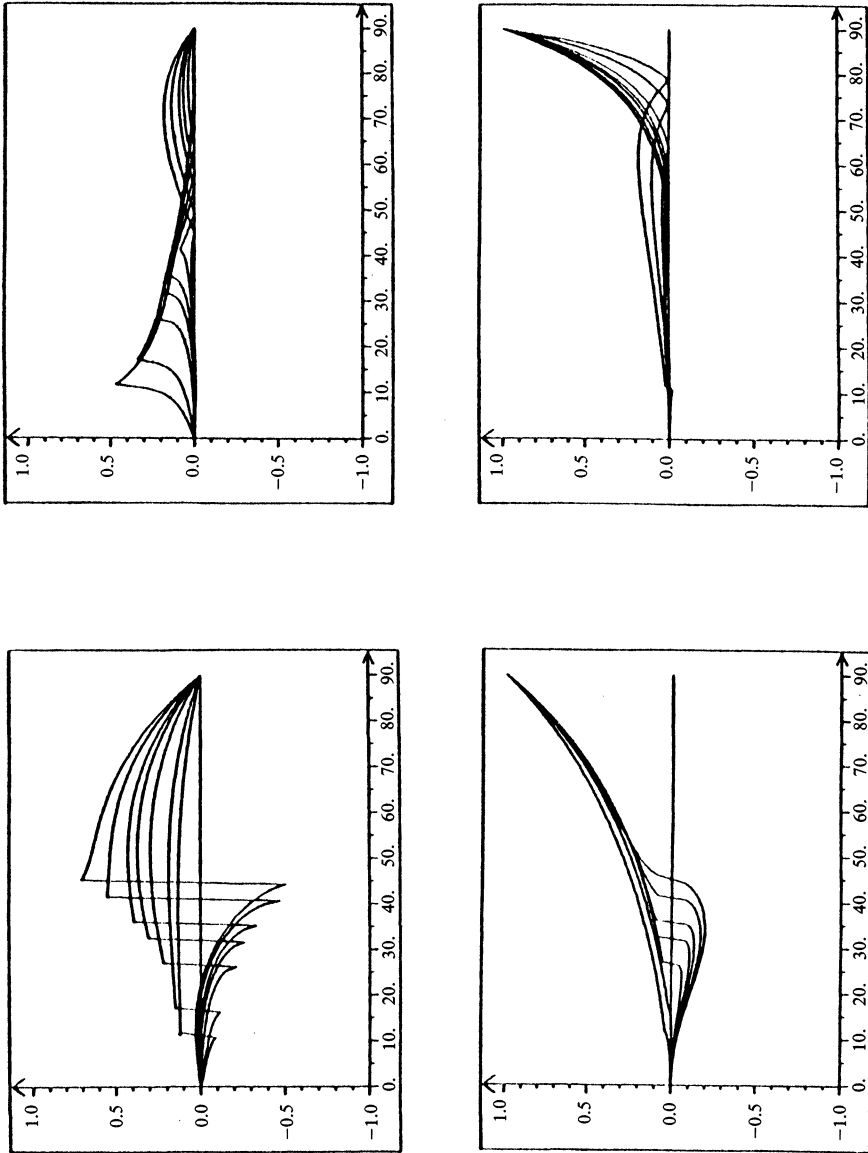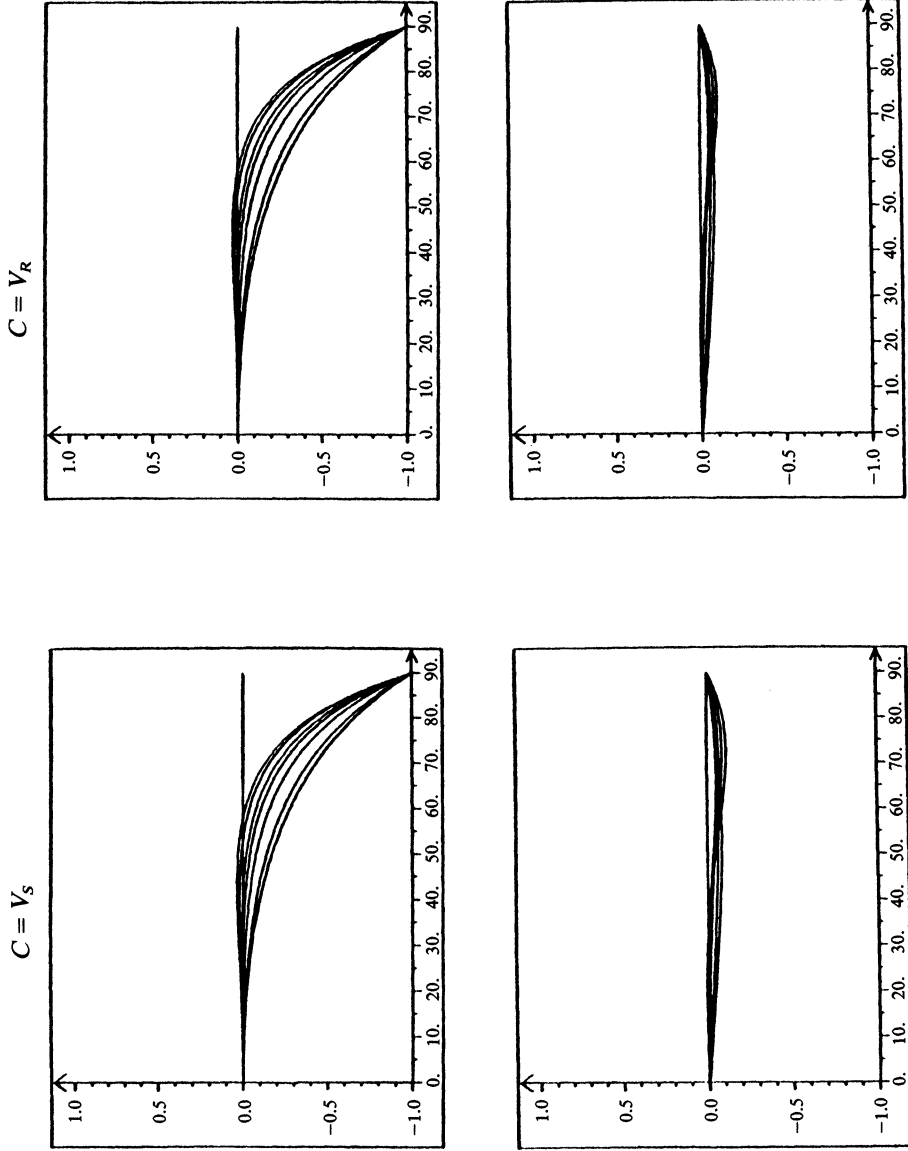
FIG. 3.1. *Reflection coefficients.*

FIG. 3.1. (cont.)

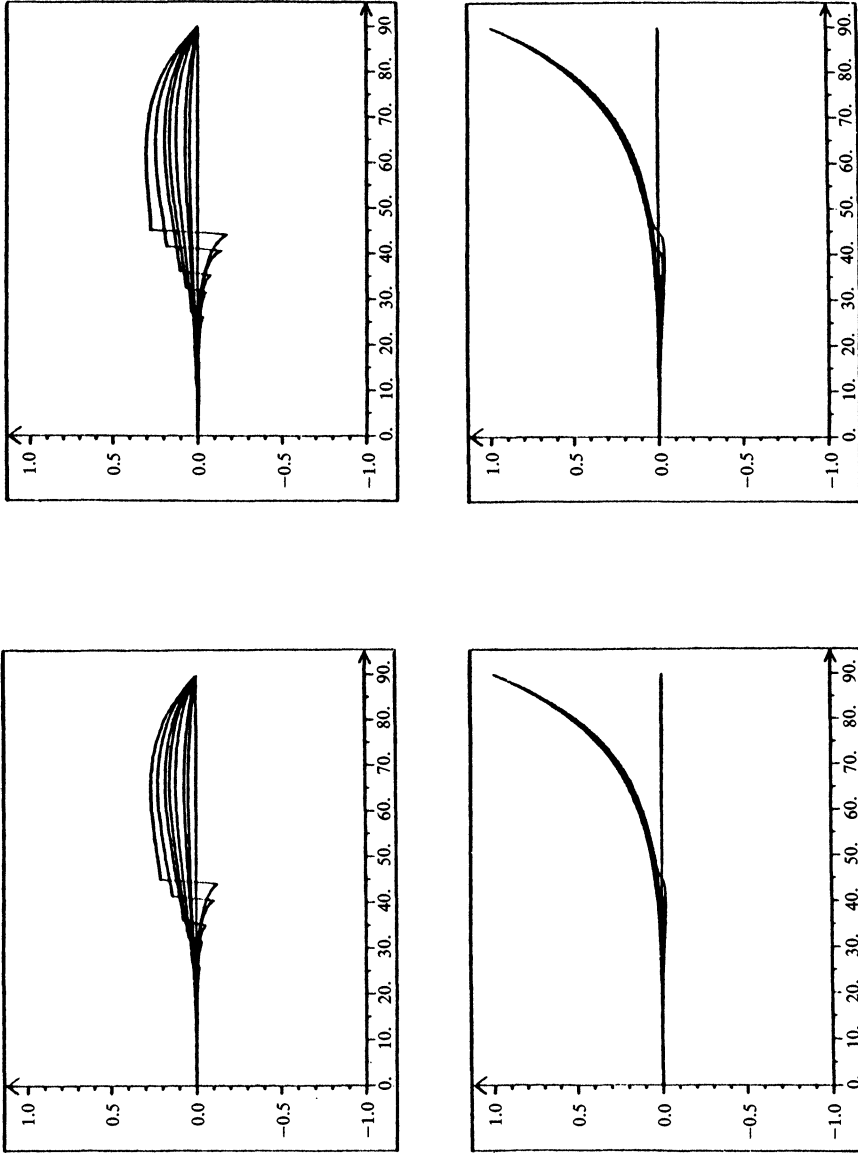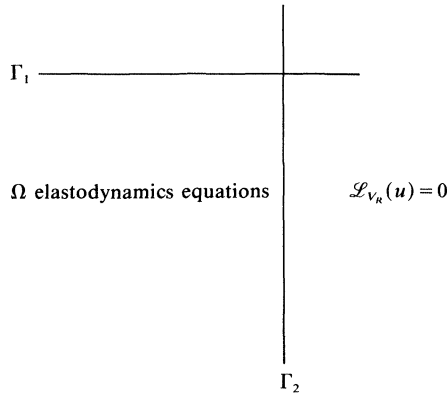FIG. 3.2. *Reflection coefficients.*

FIG. 3.2. (cont.)

Thus, all P, S, and Rayleigh waves at normal incidence are absorbed by the boundary Γ_2.

Remark. In order that Rayleigh waves traveling along the boundary Γ_1 be absorbed by the boundary Γ_2, we need to take $C = V_R$, the velocity of the Rayleigh wave. On the other hand, Theorem 3.3 indicates that it would also be of interest to take $C = V_P$ or $C = V_S$ in order to have a higher-order absorbing condition for P waves or for S waves. Thus, we are led to a defined $C = C(x_2)$ to be a smooth function of x_2, having value V_R for small x_2 but having value, say, V_P for large values of x_2, where the amplitude of the Rayleigh wave should be negligible. A rigorous analysis in the case remains to be done.

3.4. Numerical results for the boundary condition $\mathscr{L}_C(u) = 0$.

3.4.1. The discretization scheme for the boundary condition.
Here we present without analysis the discretization scheme used to obtain our numerical results. For an in-depth study of this scheme see [3].

To describe the discretization scheme for the absorbing boundary, we restrict our attention to the left half plane Ω, $x_1 < 0$, and we assume we have the boundary condition $\mathscr{L}_C(u) = 0$ on the boundary Γ, $x_1 = 0$.

As in 1.3 and 2.2, we employ an explicit scheme using $Q1$ finite elements associated with a uniform grid to solve the equations in Ω. This scheme is equivalent to a finite difference scheme, and we use a finite difference approximation to discretize the boundary condition.

The condition $\mathscr{L}_C(u) = 0$ on Γ can be rewritten as follows:

$$\left[A_0 \frac{\partial^2}{\partial t^2} + A_1 \frac{\nabla^2}{\partial t \partial x_1} + A_2 \frac{\partial^2}{\partial t \partial x_2} + A_3 \frac{\partial^2}{\partial x_2^2} + A_4 \frac{\partial^2}{\partial x_1 \partial x_2} \right] (u) = 0,$$

where the matrices A_0, A_1, A_2, A_3, and A_4 are defined by

$$A_0 = \rho \begin{pmatrix} 1 & 0 \\ 0 & 1 \end{pmatrix}, \qquad A_1 = \rho \begin{pmatrix} V_P & 0 \\ 0 & V_S \end{pmatrix},$$

$$A_2 = \rho \begin{pmatrix} 0 & (V_P^2 - 2V_S^2)/(V_P + C) \\ V_S^2/(V_S + C) & 0 \end{pmatrix},$$

$$A_3 = -\rho C \begin{pmatrix} V_S^2/(V_P + C) & 0 \\ 0 & V_P^2/(V_S + C) \end{pmatrix},$$

$$A_4 = -\rho C \begin{pmatrix} 0 & V_S^2/(V_P + C) \\ V_P^2/(V_S + C) & 0 \end{pmatrix}.$$

Thus to describe the approximation scheme it suffices to give the approximation of each of the derivatives

$$\frac{\partial^2 u}{\partial t^2}, \quad \frac{\partial^2 u}{\partial t \partial x_1}, \quad \frac{\partial^2 u}{\partial t \partial x_2}, \quad \frac{\partial^2 u}{\partial x_2^2}, \quad \frac{\partial^2 u}{\partial x_1 \partial x_2}.$$

The scheme is designed to be explicit in time, centered at time level n, and centered in space between the two last columns of the grid and to be second order in time and space. If we denote the approximation of the function $u(x_1, x_2, t)$ at time $t^n = n\Delta t$, $n = 0, 1, 2, \cdots$, at the grid point $(x_1^i, x_2^j) = (i\Delta x, j\Delta x) i = \cdots, -1, 0, 1, \cdots; j = \cdots, -2, -1, 0$, by $u_{i,j}^n$, then to obtain the value $u_{0,j}^{n+1}$, we approximate the above derivatives on the boundary Γ, $x_1 = 0$, as follows:
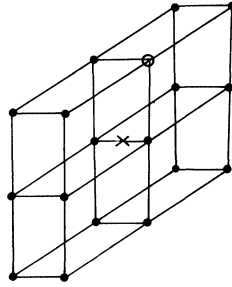
For $\partial^2 u / \partial t \partial x_1$, the standard backward difference in x_1 and centered first-order difference in t are used:

$$\frac{\partial^2 u}{\partial t^2} = \frac{1}{2} \left(\frac{u_{0,j}^{n+1} - 2u_{0,j}^n + u_{0,j}^{n-1}}{\Delta t^2} + \frac{u_{-1,j}^{n+1} - 2u_{-1,j}^n + u_{-1,j}^{n-1}}{\Delta t^2} \right).$$

For $\partial^2 u / \partial t \partial x_1$, the standard backward difference in x_1 and centered first-order difference in t are used:

$$\frac{\partial^2 u}{\partial t \partial x_1} = \left(\frac{u_{0,j}^{n+1} - u_{-1,j}^{n+1}}{\Delta x} - \frac{u_{0,j}^{n-1} - u_{-1,j}^{n-1}}{\Delta x} \right) \bigg/ 2\Delta t.$$

For $\partial^2 / \partial t \partial x_2$, the derivative in the x_2 direction is approximated by the standard centered difference, but to keep the scheme explicit while centering between $x_{0,j}$ and $x_{-1,j}$, the time derivative is approximated by the average of a forward difference at $x_{-1,j}$, and a backward difference at $x_{0,j}$:

$$\frac{\partial^2 u}{\partial t \partial x_2} = \left(\frac{u_{-1,j+1}^{n+1} - u_{-1,j-1}^{n+1}}{2\Delta x} - \frac{u_{-1,j+1}^n - u_{-1,j-1}^n}{2\Delta x} \right) \bigg/ 2\Delta t$$

$$+ \left(\frac{u_{0,j+1}^n - u_{0,j-1}^n}{2\Delta x} - \frac{u_{0,j+1}^{n-1} - u_{0,j-1}^{n-1}}{2\Delta x} \right) \bigg/ 2\Delta t.$$

The second derivative in x_2, $\partial^2 / \partial x_2^2$, is approximated by the average of the standard second difference at $x_{0,j}$ at time level n and that at $x_{-1,j}$,

$$\frac{\partial^2 u}{\partial x_2^2} = \frac{u_{0,j+1}^n - 2u_{0,j}^n + u_{0,j-1}^n}{2\Delta x^2} + \frac{u_{-1,j+1}^n - 2u_{-1,j}^n + u_{-1,j-1}^n}{2\Delta x^2}.$$

Finally, for $\partial^2 / \partial x_1 \partial x_2$, we use a centered difference in x_2 and a backward difference in x_1, all at time level n:

$$\frac{\partial^2 u}{\partial x_1 \partial x_2} = \left(\frac{u_{0,j+1}^n - u_{0,j-1}^n}{2\Delta x} - \frac{u_{-1,j+1}^n - u_{-1,j-1}^n}{2\Delta x} \right) \bigg/ \Delta x.$$

Hence, in classical notation, the difference scheme may be written as follows:

$$\tfrac{1}{2}A_0 D_+^t D_-^t (u_{0,j}^n + u_{-1,j}^n) + A_1 D_0^t D_-^{x_1}(u_{0,j}^n),$$

(3.6) $$\tfrac{1}{2}A_2 D_0^{x_2} D_+^t (u_{0,j}^{n-1} + u_{-1,j}^n) + \tfrac{1}{2}A_3 D_-^{x_2} D_+^{x_2}(u_{0,j}^n + u_{-1,j}^n)$$

$$+ A_4 D_0^{x_2} D_-^{x_1}(u_{0,j}^n) = 0, \qquad j = \cdots, \ -1, 0, 1, \cdots.$$

We point out that the case of a corner joining the absorbing boundary with a free boundary must be treated separately. Let Ω denote the lower left quarter plane, $x_1 < 0$, $x_2 < 0$, and assume that on the boundary Γ_1, $x_2 = 0$ we have the free boundary condition $\sigma \cdot \nu = 0$ and on the boundary Γ_2, $x_1 = 0$, the absorbing condition $\mathcal{L}_C(u) = 0$. Then some of the terms in (3.6) are defined only for $j < 0$, and indeed the question arises as to whether there needs to be a special treatment mathematically as well as numerically for such a corner. Thus, following the development in [1], where the corner condition for a corner joining two absorbing boundaries for the wave equation is treated, we are led to construct a condition for the corner by assuming that both the free and the absorbing boundary conditions, as well as the equations of elastodynamics, hold at the corner, and then use this assumption to eliminate the troublesome derivatives. For the resulting condition, as well as its numerical treatment, we again refer the reader to [3].

3.4.2. Presentation of the numerical results.

Here we repeat the experiments given in 1.3 and 2.2, changing the absorbing boundary condition. The results are presented in the form of seismograms. As before, the receptors have been placed along the right half of the upper boundary, and each simulation will generate two groups of seismograms, the first depicting the horizontal components of the displacements and a second one the vertical components.

We normalize all these seismograms with the same value in order to exactly compare the reflections generated by each boundary condition. However, we shall use a greater gradient of amplification than in 1.3 and 2.2 because of the small values of the reflections obtained with the boundary condition $\mathcal{L}_C(u) = 0$.

In order to illustrate the threshold conclusions at § 3.2, we shall present the results for four simulations where we have successively used on the vertical edges:

  (i) The first-order absorbing boundary condition $\mathcal{L}_1(u) = 0$, (Figs. 3.3 and 3.4);
  (ii) The absorbing boundary condition $\mathcal{L}_C(u) = 0$ with $C = V_P$, (Figs. 3.5 and 3.6);
  (iii) The absorbing boundary condition $\mathcal{L}_C(u) = 0$ with $C = V_S$, (Figs. 3.7 and 3.8);
  (iv) The absorbing boundary condition $\mathcal{L}_C(u) = 0$ with $C = V_R$, (Figs. 3.9 and 3.10).

Our first observation is that condition $\mathcal{L}_C(u)$, for each choice of C, is clearly an improvement over $\mathcal{L}_1(u)$ with regard to the absorption of each kind of wave.

When $C = V_P$ (Figs. 3.5 and 3.6), we no longer see any trace of a wave along the lines D_{PP} and D_{PR}, i.e., the operator $\mathcal{L}_{V_P}$ seems to have completely absorbed the P wave. However, in this case we can clearly observe waves along the lines D_{RP} and D_{RR}, indicating a reflection of the Rayleigh wave and a conversion of the Rayleigh wave to a P wave.

On the contrary, when we choose $C = V_R$ (Figs. 3.9 and 3.10), we note a much better absorption of the Rayleigh wave while there remain small reflections due to the P wave.

Finally, we note that the choice $C = V_S$ (Figs. 3.7 and 3.8), for the example given here, presents little change from the choice $C = V_R$ since the difference between V_S and V_R is small. However, in other examples we tested, where V_R and V_S were not so close, the Rayleigh wave was much better absorbed by the condition $\mathcal{L}_{V_R}$ than by $\mathcal{L}_{V_S}$.
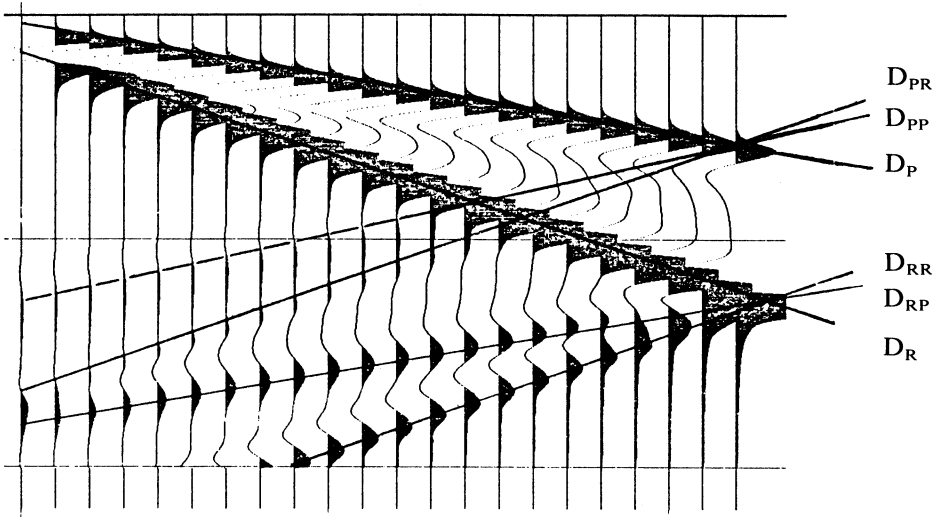
FIG. 3.3. $\mathscr{L}_1(u) = 0$: *Horizontal displacement. Gradient of amplification* $= 3 \times 10^{-4}$.
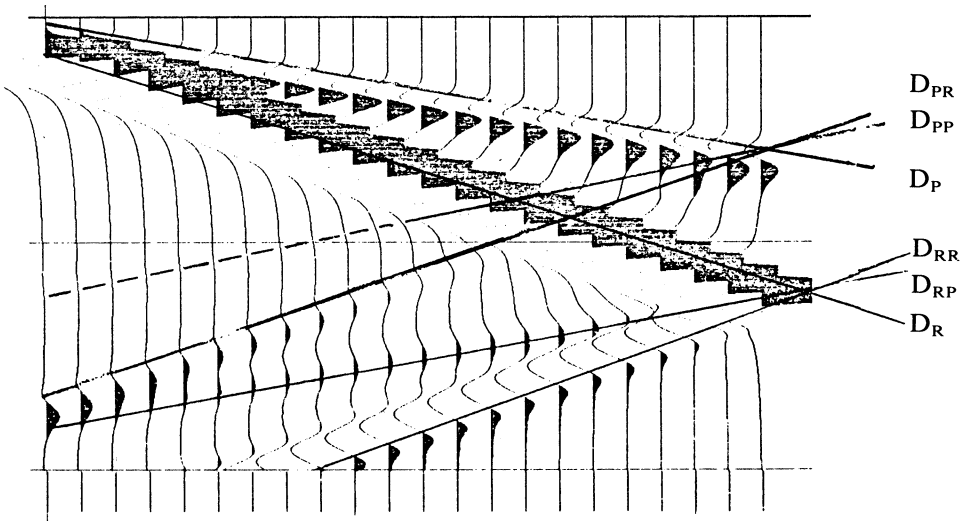

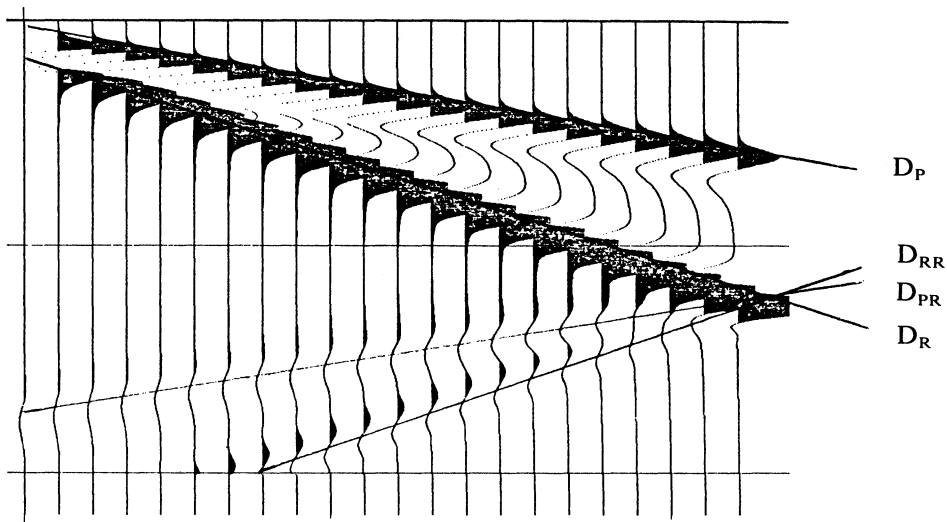FIG. 3.4. $\mathscr{L}_1(u) = 0$: *Vertical displacement. Gradient of amplification* $= 3 \times 10^{-4}$.

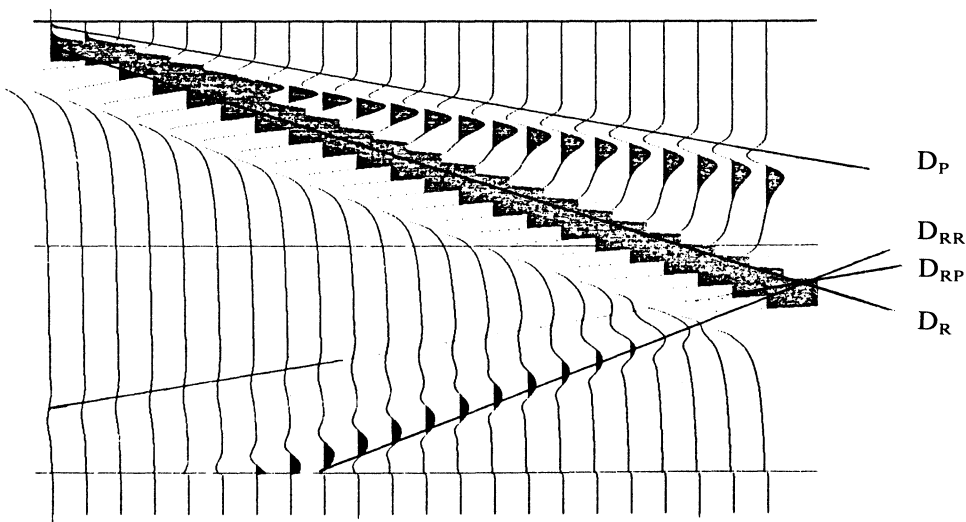FIG. 3.5. $\mathscr{L}_{V_P}(u) = 0$: *Horizontal displacement. Gradient of amplification* $= 3 \times 10^{-4}$.

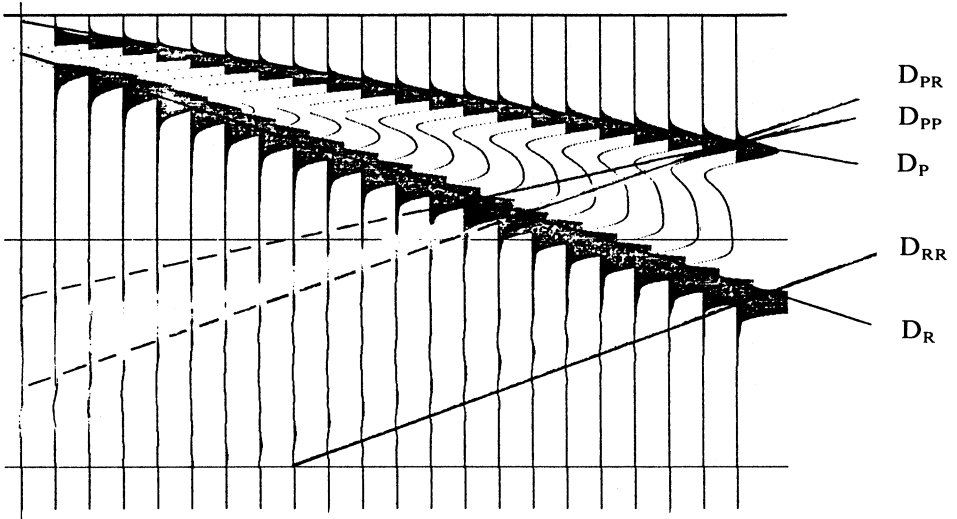FIG. 3.6. $\mathscr{L}_{V_P}(u) = 0$: *Vertical displacement. Gradient of amplification* $= 3 \times 10^{-4}$.

FIG. 3.7. $\mathscr{L}_{V_S}(u) = 0$: *Horizontal displacement. Gradient of amplification* $= 3 \times 10^{-4}$.
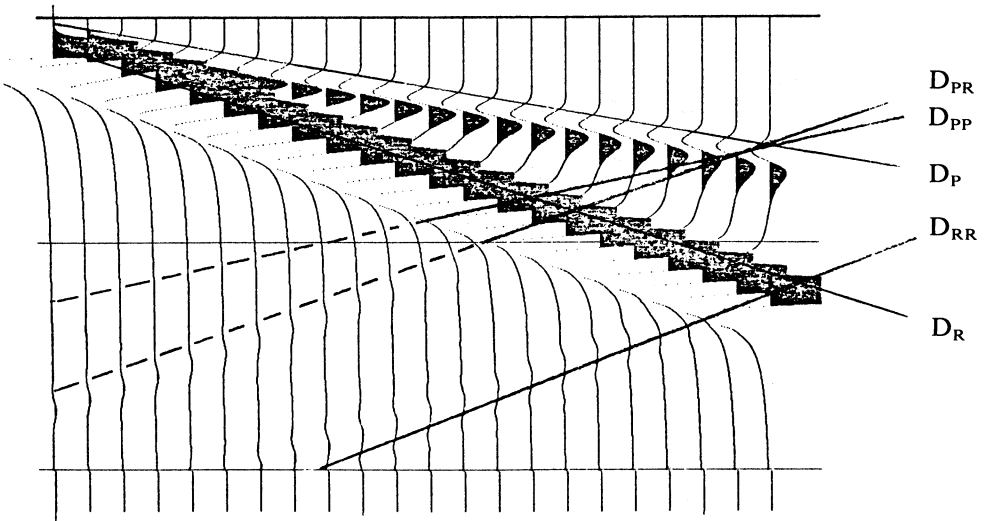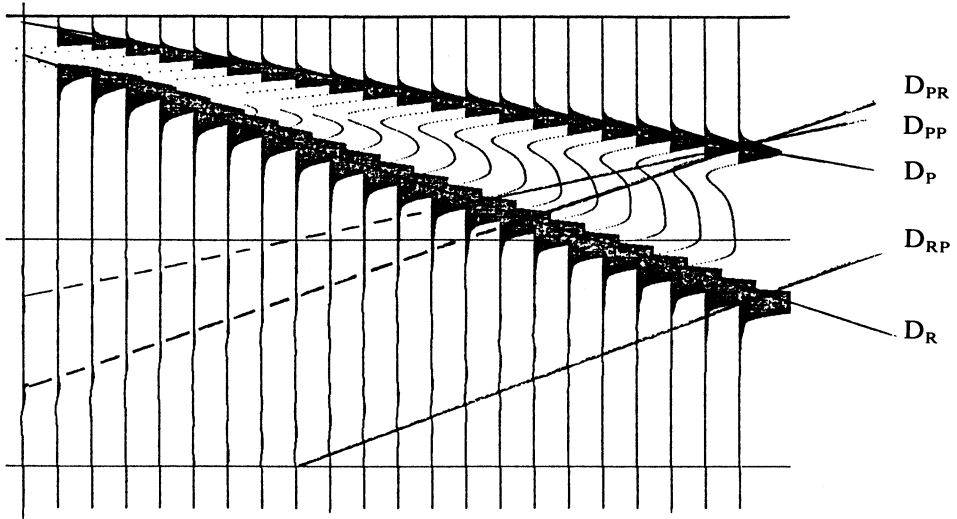

FIG. 3.8. $\mathscr{L}_{V_S}(u) = 0$: *Vertical displacement. Gradient of amplification* $= 3 \times 10^{-4}$.

D_{PR}
D_{PP}
D_P

D_{RP}

D_R

FIG. 3.9. $\mathscr{L}_{V_R}(u) = 0$: *Horizontal displacement. Gradient of amplification* $= 3 \times 10^{-4}$.

D_{PR}
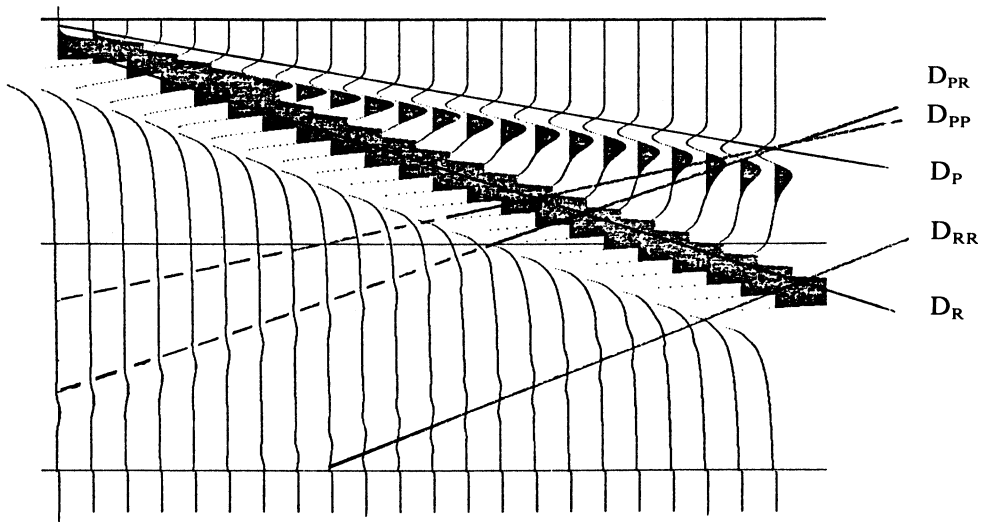D_{PP}

D_P

D_{RR}

D_R

FIG. 3.10. $\mathscr{L}_{V_R}(u) = 0$: *Vertical displacement. Gradient of amplification* $= 3 \times 10^{-4}$.

Hence, we conclude that by varying the value of the speed C, we can select the type of wave to be absorbed. Particularly in our case, we would choose $C = V_R$ in order to most nearly eliminate the reflection due to the Rayleigh wave propagating along the surface.

3.5. Conclusion. The boundary condition $\mathscr{L}_{V_R}$ we derived in this article gives good results as shown by the numerical experiments of § 3.4. This condition is in particular very efficient for eliminating the parasitic phenomena due to Rayleigh waves, according to the theoretical results. It would be interesting to investigate the generalization of this condition to the three-dimensional case.

REFERENCES

[1] A. BAMBERGER, P. JOLY, AND J. ROBERTS, *Second order absorbing boundary conditions for the wave equation: a solution for the corner problem.* INRIA Report no. 644; SIAM J. Appl. Math., submitted.

[2] A. BAYLISS AND E. TURKEL, *Radiation boundary conditions for wave-like equations.* Comm. Pure Appl. Math., 33 (1980), pp. 707–725.

[3] B. CHALINDAR, *Conditions aux limites absorbantes pour les équations de l'élastodynamique linéaire,* Thèse, Université de St. Etienne (1988).

[4] R. CLAYTON AND B. ENGQUIST, *Absorbing boundary conditions for acoustic and elastic wave equations,* Bull. Seismol. Soc. Amer., 67 (1977), pp. 1529–1540.

[5] M. COHEN AND P. C. JENNINGS, *Silent boundary methods for transient analysis,* Comput. Methods for Transient Analysis, 1 (1983), pp. 301–357.

[6] B. ENGQUIST AND A. MAJDA, *Radiation boundary conditions for acoustic and elastic wave calculations,* Comm. Pure. Appl. Math., 32 (1979), pp. 313–357.

[7] L. HALPERN, *Etude de conditions aux limites absorbantes pour des schémas numériques relatifs à des équations hyperboliques linéaires,* Thèse de 3ème Cycle, Université Paris VI, 1980.

[8] J. LYSMER AND R. L. KUHLMEYER, *Finite dynamic model for infinite media,* J. Engrg. Mech. Div., Proc. ASCE 95 EM4 (1969), pp. 859–877.

[9] D. H. RUDY AND J. C. STRIKWERDA, *A nonreflecting outflow boundary condition for subsonic Navier-Stokes calculations,* J. Comput. Phys., 36 (1980), pp. 55–70.